



## Research

**Cite this article:** Weinell JL, Burbrink FT, Das S, Brown RM. 2024 Novel phylogenomic inference and ‘Out of Asia’ biogeography of cobras, coral snakes and their allies. *R. Soc. Open Sci.* **11**: 240064.

<https://doi.org/10.1098/rsos.240064>

Received: 11 January 2024

Accepted: 31 May 2024

**Subject Category:**

Organismal and evolutionary biology

**Subject Areas:**

evolution

**Keywords:**

Africa, Elapidae, Elapoidea, Cyclocoridae, Lamprophiidae, phylogenomics

**Author for correspondence:**

Jeffrey L. Weinell

e-mails: [jweine2@gmail.com](mailto:jweine2@gmail.com); [jweinell@amnh.org](mailto:jweinell@amnh.org)

<sup>†</sup>Present address: Department of Herpetology, American Museum of Natural History, 200 Central Park West, New York, NY, USA.

Electronic supplementary material is available online <https://doi.org/10.6084/m9.figshare.c.7385057>.

# Novel phylogenomic inference and ‘Out of Asia’ biogeography of cobras, coral snakes and their allies

Jeffrey L. Weinell<sup>1,2,†</sup>, Frank T. Burbrink<sup>2</sup>, Sunandan Das<sup>3</sup> and Rafe M. Brown<sup>1</sup>

<sup>1</sup>Department of Ecology and Evolutionary Biology and Biodiversity Institute, University of Kansas, 1345 Jayhawk Blvd, Lawrence, KS 66045, USA

<sup>2</sup>Department of Herpetology, American Museum of Natural History, 200 Central Park West, New York, NY 10024, USA

<sup>3</sup>Ecological Genetics Research Unit, Organismal and Evolutionary Biology Research Programme, Faculty of Biological and Environmental Sciences, University of Helsinki, Helsinki 00014, Finland

ORCID: JLW, [0000-0002-9568-0672](https://orcid.org/0000-0002-9568-0672); FTB, [0000-0001-6687-8332](https://orcid.org/0000-0001-6687-8332); SD, [0000-0002-1597-1147](https://orcid.org/0000-0002-1597-1147); RMB, [0000-0001-5338-0658](https://orcid.org/0000-0001-5338-0658)

Estimation of evolutionary relationships among lineages that rapidly diversified can be challenging, and, in such instances, inaccurate or unresolved phylogenetic estimates can lead to erroneous conclusions regarding historical geographical ranges of lineages. One example underscoring this issue has been the historical challenge posed by untangling the biogeographic origin of elapid snakes, which includes numerous dangerously venomous species as well as species not known to be dangerous to humans. The worldwide distribution of this lineage makes it an ideal group for testing hypotheses related to historical faunal exchanges among the many continents and other landmasses occupied by contemporary elapid species. We developed a novel suite of genomic resources, included worldwide sampling, and inferred a robust estimate of evolutionary relationships, which we leveraged to quantitatively estimate geographical range evolution through the deep-time history of this remarkable radiation. Our phylogenetic and biogeographical estimates of historical ranges definitively reject a lingering former ‘Out of Africa’ hypothesis and support an ‘Out of Asia’ scenario involving multiple faunal exchanges between Asia, Africa, Australasia, the Americas and Europe.

# 1. Introduction

How, why and when geographic distributions of lineages have changed through time are primary questions motivating the conceptual unification of phylogenetic systematics, macroecology and Earth history in the multi-disciplinary field of modern biogeography. Characteristics of geography, climate, species interactions and historical contingency have all been implicated in determining present-day geographic ranges of species [1]. Tests of biogeographic hypotheses related to historical faunal exchanges require well-documented information about the geographic ranges of species, knowledge of Earth history and historical environmental changes, and robust analytical methods for inferring evolutionary relationships and historical geographic ranges of lineages. As a result of centuries of field-based exploration and biogeographical research [2–6], geographic ranges have been broadly characterized, at least at a continental resolution, for most known terrestrial vertebrate species [7,8] and evolutionary relationships have been inferred for many vertebrate lineages as a result of molecular phylogenetic studies over the last half-century [9–15]. However, for groups within which little is known about species diversity, evolutionary relationships or geographic ranges of lineages—commonly known as Linnean, Darwinian and Wallacean shortfalls [16–19]—biogeographic origins are often unknown and can be hard to accurately estimate.

One such group is the snake superfamily Elapoidea, which includes over 700 species in nine families and is geographically distributed in tropical and subtropical regions on all the planet's major continents and in marine habitats of Indian and Pacific oceans (figure 1) [20–22]. The group's biogeographic origin, however, has remained uncertain. Earlier studies have supported an African origin for this lineage—implying its ancestral expansion 'Out of Africa'—and highlighted its rapid diversification in Africa [21–29]. An African origin has also been supported for numerous additional vertebrate groups presently or historically distributed on multiple continents [30–37]. One significant barrier that has precluded robust quantitative biogeographical investigation of Elapoidea persists: a strongly supported, time-calibrated estimate of evolutionary relationships, including all extant major (family-rank level) lineages and sublineages, has remained unavailable.

Here, we used a targeted sequence capture approach to produce a phylogeny that samples all major elapoid lineages and outgroups. We used this phylogenomic tree and information from the fossil record of snakes to estimate a strongly supported, time-calibrated phylogenetic framework for implementation of modern biogeographical inference. We generated the most comprehensive biogeographical inference performed to date with respect to taxonomic coverage, number of loci and the use of powerful, statistically coherent methods. Using our results from biogeographic analyses, we assess previous hypotheses related to historical faunal exchange and the 'Out of Africa' scenario supported by previous phylogenetic, biogeographic and palaeontological analyses [21,25,38]. Results supporting ancestral range expansions into or out of Africa before formation of a land bridge connection between this continent and Eurasia would necessarily indicate that such expansions probably stemmed from historical oceanic dispersal events.

# 2. Material and methods

## 2.1. Sequence capture dataset

We sampled 66 individuals from 65 species in 52 genera and 22 families of snakes, from DNA isolated from ethanol-preserved tissue samples or from previously assembled genomes (electronic supplementary material, table S1). Tissues were collected by numerous individuals (electronic supplementary material) during field expeditions (1990–2018) and deposited in the tissue collections at the University of Kansas Biodiversity Institute, University of Texas at El Paso or Villanova University (Villanova, PA).

We targeted 3128 loci and 1 517 011 nucleotides (nt) for capture with a MyBaits-20 custom RNA probe kit (Arbor BioSciences) containing 20 020 120 nt probes and 2X probe tiling. Target loci included 1652 rapidly evolving exons (REEs), 907 UCEs, 328 ddRAD-like (*in silico* identification), 27 major histo-compatibility, 119 vision-associated and 95 scalation-associated loci (electronic supplementary material; Open Science Framework project krhx3). Targeted regions of REEs included 121–7501 nt, one or more entire exons and partial upstream, downstream or both up- and down-stream exon-flanking regions. Sequence capture libraries were dual-indexed and paired-end sequenced (150 bp inserts) on an Illumina HiSeq X sequencer (NovoGene).

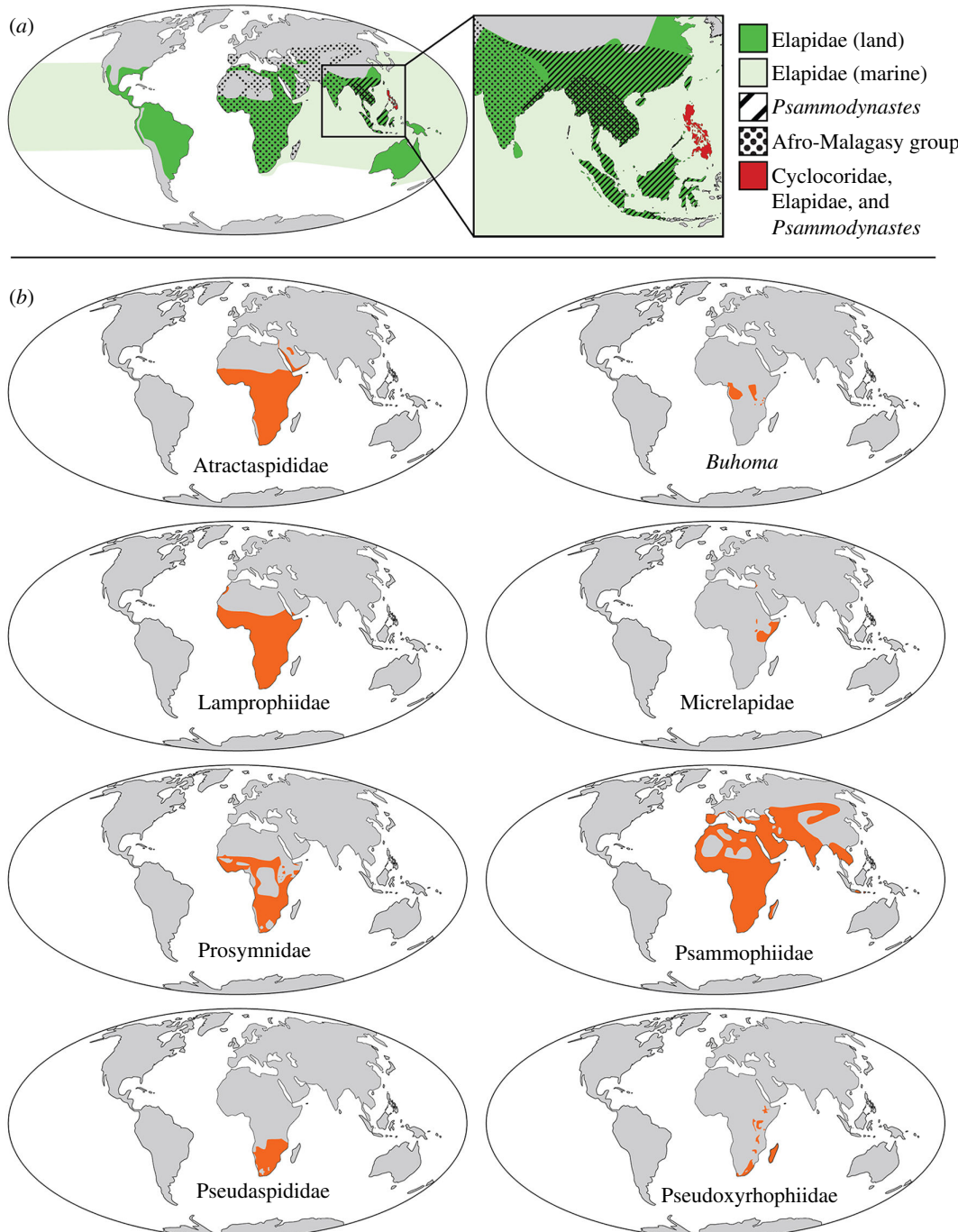


**Figure 1.** Geographic extents of major lineages of Elapoidea; (a) geographic distributions for Cyclocoridae (red), Elapidae (green or red), *Psammodynastes* (diagonal black stripes or red) and the group comprising non-elapid Afro-Malagasy lineages (black circle pattern); (b) geographic extent (orange) for each major lineage (family-rank or similar) of the Afro-Malagasy group.

We demultiplexed fastq files with ‘demuxbyname’ from BBMap [39], trimmed adapters with FASTP [40], filtered contaminant reads by comparison with a database of common contaminants with BBMap [41,42], removed duplicate reads with ‘dedupe’ tool in BBTools and merged read pairs with BBMerge [43]. To de novo assemble reads into contigs, we used SPAdes 3.12 [44] with multiple k-mer values and dipSPAdes in SPAdes [45] for polymorphic read assembly. We masked low complexity and repeat regions with repeatMasker 4.1.0 [46]. To annotate contigs, we used BLASTn from BLAST+2.9 to match contigs against probe target reference sequences, filtered matches with bitscore < 50, and binned contigs into disjoint clusters with R package ‘igraph’ and SeqKit 2 [47–49].

To obtain orthologous sequences from previously assembled genomes (electronic supplementary material, table S1) for each locus in our novel sequence capture dataset, we aligned novel sequences

using MAFFT 7.310 [50] and generated a consensus sequence of the alignment result using R package 'Biostrings' 2.60.2 [51]; searched for matches to the consensus sequence in 20 kb windows of genome assembly scaffolds using BLASTn [52]; pairwise-aligned sequences with a strong match (bitscore > 50); trimmed contiguous sites at ends of each pairwise alignment containing missing data for either sequence; retained the genome-derived sequence from each trimmed pairwise alignment; and removed gaps. We excluded loci, when multiple homologous regions were identified in the same genome assembly, and we considered sequences of included loci to be orthologous. To generate every single locus alignment used for phylogenetic estimation of gene trees, we aligned sequence capture and genome-derived orthologs using MAFFT 7.310, and trimmed each alignment down to the largest contiguous region containing 90% complete data. To generate our concatenation dataset, we concatenated single locus alignments using SeqKit 2 and R package 'Biostrings' 2.60.2 [49,51,53].

## 2.2. Sanger dataset

To estimate a chronogram with dense taxonomic sampling for our biogeographic analyses, we sampled genetic data for 450 individuals from 434 species of snakes in 379 genera and 24 families and non-nominate subfamilies. We compiled DNA sequences from GenBank ( $n = 428$  individuals) and generated novel genetic data from ethanol-preserved tissue samples of 22 individuals of 21 species and genera (electronic supplementary material, table S2). Sampled loci included the mitochondrial protein-coding genes cytochrome b (CYTB), and five nuclear-encoded genes: brain-derived neurotrophic factor (BDNF), oocyte maturation factor mos (C-MOS), 3'-nucleotidase (NT3), recombination activating 1 (RAG1) and recombination activating 2 (RAG2). To extract and purify genomic DNA, we digested tissues using Proteinase K enzyme and used a Maxwell® Rapid Sample Concentrator Instrument with Maxwell® 16 Tissue DNA Purification Kit (Promega Corporation). We used 34 cycles of polymerase chain reaction (PCR) with annealing temperature 49°C ( $\pm 1\text{--}5^\circ\text{C}$ ) and previously designed PCR and sequencing primers (electronic supplementary material, table S3) to amplify 1350 base pairs (bp) of CYTB and 580 bp of C-MOS. Amplified products were visualized using gel electrophoresis on 1.5% agarose gels. Purification of PCR products, cycle sequencing, cycle sequencing cleanups and nucleotide sequence determination were conducted with standard GeneWiz protocols®. We de novo assembled and edited Sanger sequences using GENEIOUS® 6.1 and GENEIOUS PRIME® 2021.2.2, aligned sequences separately for each locus with MAFFT 7.310 [50,54] and used GENEIOUS PRIME® and SeqKit 2 [49] to trim alignment ends, identify reading frames, filter out individuals with early stop codons in protein coding regions and concatenate alignments.

## 2.3. Phylogenetic inference

To estimate maximum likelihood (ML) gene trees from our single locus alignments and ML phylogeny from our concatenated sites alignment, we ran IQ-TREE 2.2 [55] with node support assessed from 1000 ultrafast bootstraps (UFBoot) [56]. For estimation of gene trees from single locus alignments, sites were partitioned into the disjoint set of protein-coding and non-coding regions determined by mapping protein-coding annotations from genome annotation files to our single locus alignments (electronic supplementary material; Open Science Framework, project krhx3), and we used option '-m TESTMERGE' of MODELFINDER in IQ-TREE 2.1.3 to estimate the optimal partitioning scheme and to identify the best-fit substitution model for each partition. For phylogenetic estimation using our concatenated informative sites alignment, sites were unpartitioned and we used option '-m TEST' of MODELFINDER in IQ-TREE 2.1.3 to identify the best substitution model. We considered UFBoot  $\geq 95$  and SH-aLRT  $\geq 80$  to be strong support for monophyly [55].

To infer the species tree with local posterior probability (PP) values of node support, we used ASTRAL-III 5.6.1 [57] and quartet trees sampled from our estimated gene trees with low support nodes (UFBoot  $\leq 10$ ) collapsed into polytomies; we considered PP  $> 0.95$  to be strong support for monophyly [57]. We used R packages 'ape' 5.6.1 [58] and 'Quartet' 1.2.2 [59] to estimate metrics of similarity and dissimilarity among gene, species and concatenation tree topologies, including Robinson–Foulds Distance (RFD), Strict Joint Assertions and Quartet Divergence (QDiv).

We inferred phylogenetic relationships using our Sanger sequence alignment and IQ-TREE 2.1.3 and optimal site-partitioning scheme estimated using MODELFINDER implemented in IQ-TREE with option '-m TESTMERGEONLYNEW'. During phylogenetic inference, we used a highly resolved topological constraint tree congruent at the family-rank level with our inferred species tree and with

additional topological constraints corresponding to a curated list of clades strongly supported in previous phylogenetic studies (electronic supplementary material; Open Science Framework project krhx3). To initiate tree optimization, we used a starting tree with topology generated by randomly resolving multichotomies in our constraint tree using function ‘multi2di’ from R package ‘ape’ 5.6.1 [58]. For unconstrained nodes, we assessed node support from 1000 UFBoot and 1000 replicates for Shimodaira–Hasegawa-like approximate likelihood ratio testing [56,60].

## 2.4. Divergence time estimation

We estimated divergence times for our inferred ‘sequence capture species tree’ and ‘Sanger ML tree’ using RelTime-ML [61–63] in MEGA 11 [63]; an alignment with 10 000 sites randomly sampled without replacement from our sequence capture dataset (for analysis with inferred species tree) or the full Sanger sequence alignment (for analysis with inferred Sanger tree); and five node-calibration age constraints with lognormally distributed probability densities generated using information from the fossil record (electronic supplementary material, table S4). Calibrated nodes and confidence intervals (CIs) of calibrated node age probability densities included: Viperinae stem node (CI: 24.0–51.2 Ma); Elapidae stem node (CI: 26.8–54.0 Ma); Dipsadidae stem node (CI: 14.4–41.6 Ma); Colubroidea stem node (CI: 37.1–64.3 Ma); and the stem node of the clade that includes descendants of the most recent common ancestor (MRCA) of *Hydrophis* and *Laticauda* (CI: 11.9–39.1 Ma).

## 2.5. Historical hybridization and incomplete lineage sorting

To test for historical hybridizations, we estimated phylogenetic networks from gene concordance factors (gCFs) using SNaQ [64] implemented in the JULIA package ‘PhyloNetworks’ 0.14.3 [65,66]. We compared quartet trees sampled from our gene trees against the set of quartets obtained by quartet decomposition of the species tree to estimate gCFs, ran SNaQ 10 times under each *a priori* maximum number of reticulations (which we varied from 0 to 10), and retained the maximum pseudolikelihood network for each number of reticulations [64,67]. To estimate the optimal number of reticulations from the set of maximum pseudolikelihood networks, we used DjumP and DDSE algorithms in R package ‘capushe’ 1.1.1 [68], which calculate slope heuristics considering model complexity and change in pseudolikelihood with each increase in number of reticulations [69]. We considered the optimal phylogenetic network to be the maximum pseudolikelihood network that had the outgroup lineage correctly inferred as the outgroup, and number of the reticulations equal to the inferred optimal number of reticulations. We also considered historical hybridization to be supported if the optimal phylogenetic network contained a hybrid edge.

To assess if our phylogenetic results deviated from expectations of ILS, we estimated gene discordance factors (gDF1 and gDF2) and site discordance factors (sDF1 and sDF2) for internal nodes of our species tree and the phylogeny estimated from our concatenated-locus alignment, using IQ-TREE 2.1.3, our single-locus alignments and quartets sampled from our estimated gene trees. We conducted  $\chi^2$ -tests of the hypothesis of no difference between sDF1 and sDF2, and no difference between gDF1 and gDF2, with significance considered at the 0.05 level [70,71]. Following the recommendation of Lanfear [70], we binned putatively unlinked sites from our concatenated sites alignment by locus, bootstrap sampled one site per locus (100 bootstraps) and estimated site concordance factor (sCF) and sDFs from each bootstrap ‘unlinked sites alignment’ relative to our phylogenetic trees, and repeated  $\chi^2$ -tests on each bootstrapped sample to determine robustness. Significant  $\chi^2$ -test results were considered evidence against ILS-derived discordance [70], and when combined with a low sCF or low gCF, as evidence suggesting ancestral hybridization.

## 2.6. Biogeographic inference

We inferred historical geographic ranges using BioGeoBEARS 1.1.2 [72,73], our Sanger chronogram pruned to one tip per genus of superfamilies Colubroidea and Elapoidea, and a geographic distribution dataset [74] compiled from relevant literature sources and online databases [7,20,75–82]. We pruned all but one species lineage per genus and treated the geographic distribution of each retained lineage as equal to the total range of the corresponding genus.

We coded geographic distributions as either present or absent in six regions (electronic supplementary material, figure S1), including five physiogeographic land regions (Africa, Americas, Asia, Australasia and Europe) and one marine region encompassing extant sea snake distributions (i.e. Indian and Pacific oceans). Within the 'Africa' region, we included continental Africa, Madagascar and most of the Arabian Plate in the Middle East. We considered continental North and South America and islands of the Caribbean, western Atlantic and eastern Pacific oceans to comprise a single 'Americas' region. The division between 'Asia' and 'Europe' was considered to occur approximately where the Turgai Strait probably separated these continents until 45–29 Ma [83,84]. We included islands of the Sunda Shelf and the Philippines within our concept of 'Asia'. Within 'Australasia', we included continental Australia and Sahul Shelf and southwestern Pacific islands. We used these regions for biogeographic analyses because they are thought to have existed as distinct biogeographical and physiogeographical areas for most of the time hypothesized to span elapoid evolutionary history (less than or equal to approx. 30 Ma).

During biogeographical analyses, we used six geographic range evolution models: (i) Dispersal-Extinction-Cladogenesis (DEC), (ii) DEC+J, (iii) DIVALIKE, (iv) DIVALIKE+J, (v) BAYAREALIKE, and (vi) BAYAREALIKE+J models, which differ in the types of range evolution processes that can occur during cladogenesis [72,73]. The BAYAREALIKE model does not allow range evolution to occur during cladogenesis; the DEC model allows vicariance or partial sympatric speciation if either daughter lineage occupies a single region. The DIVALIKE model allows vicariant speciation even if both daughter lineages have ranges spanning multiple regions, and sympatric speciation if the ancestor occupies a single area. The models DEC+J, DIVALIKE+J and BAYAREALIKE+J allow founder speciation, whereby one daughter lineage acquires a narrow range not occupied by the ancestor, and range evolution processes allowed by DEC, DIVALIKE and BAYAREALIKE models, respectively [72,73]. Ree and Sanmartín [85] warned against using statistical model selection to compare DEC and DEC+J models against other biogeographic models, whereas Matzke [86] considered such statistical model selection as valid. We considered the optimal biogeographic model to have the lowest Akaike information criterion (AIC) [87] during statistical model selection. To avoid overinterpretive reliance on a single biogeographic estimate and implied evolutionary process, we compared ancestral geographic ranges estimated under each suboptimal biogeographic model with our results recovered under the optimal model.

### 3. Results

#### 3.1. Sequence data

Using targeted sequence capture, we obtained new genetic data for 34 individuals from 32 species (electronic supplementary material, table S1), and our genetic datasets used for phylogenetic analyses included 3066 single-locus alignments and a concatenated-loci alignment with 66 individuals, 15 301 560 sites, and 77% total missing or ambiguous data (Open Science Framework, project krhx3). Number of loci sampled per individual ranged from 2041 (*Boa constrictor*) to 2717 (*Hologerrhum philippinum*). Single-locus alignments included 4–66 sequences (median 59), 1–35 novel sequences (median 32), 528–58 675 sites (median 3697), 7–9733 informative sites (median 783) and 0.05–92.5% total missing or ambiguous data (median 65.12%); alignment length and per cent missing data were both positively correlated with number of aligned sequences ( $p << 0.05$ ;  $R^2 = 0.021$  and 0.062, respectively).

Our Sanger genetic dataset included CYTB sampled for all individuals ( $n = 450$ ; 1069 sites), and nuclear loci were sampled for subsets of individuals: BDNF ( $n = 24$ ; 673 sites); C-MOS ( $n = 225$ ; 588 sites); NT3 ( $n = 29$ ; 516 sites); RAG1 ( $n = 33$ ; 1000 sites); and RAG2 ( $n = 36$ ; 714 sites). The concatenated sequence alignment contained 4560 sites and 69.3% missing or ambiguous data. Novel Sanger data included DNA sequences for 22 individuals of 21 species for loci CYTB ( $n = 22$ ) and C-MOS ( $n = 21$ ) and can be accessed in GenBank (electronic supplementary material, table S2).

#### 3.2. Phylogenetic inference

Results from our ML phylogenetic analyses of individual loci in our sequence capture dataset included gene trees that were strongly supported at 0–100% of nodes (median 45.3%), and node support was significantly correlated with alignment length, number of aligned individuals and number

of informative sites ( $p << 0.05$ ); 402 gene trees included all 66 individuals and had low to moderate topological variation (mean pairwise QDiv = 0.816; range = 0.408–0.987). Gene trees recovered Elapoidea as either monophyletic (51.8%), paraphyletic ( $n = 47.9\%$ ) or monophyly was indeterminate ( $n = 0.3\%$ ) owing to limited sampling (i.e. one or no ingroup taxa sampled, or no outgroup sampled); Lamprophiidae: 11.5% monophyletic, 85.5% paraphyletic, 3% indeterminable; Elapidae: 81.7% monophyletic, 16.1% paraphyletic, 2.2% indeterminable; Cyclocoridae: 63.4% monophyletic, 33.1% paraphyletic and 3.5% indeterminable; *Psammodynastes*: 70.1% monophyletic, 4.2% paraphyletic, 25.6% indeterminable; non-elapid Afro-Malagasy elapoids: 15.3% monophyletic, 82% paraphyletic, 2.7% indeterminable.

Our estimated species tree and ML concatenation tree (figure 2) were each strongly supported at most nodes (PP  $\geq 0.95$  at 94% of nodes of species tree; UFBoot  $\geq 95$  at 92% of nodes of concatenation tree) and had highly similar, but not identical, topologies (RFD = 20; QDiv = 0.99). Our phylogenetic results strongly supported a clade composed of all non-elapid Afro-Malagasy elapoid lineages (figure 2), hereafter simply called the ‘Afro-Malagasy group’, composed of Atractaspididae, Lamprophiidae, Micrelapidae, Psammophiidae, Pseudaspididae, Pseudoxyrhophiidae, Prosymnidae and *Buhoma*.

The species tree analysis inferred a sister relationship between Natricidae and the lineage comprising Dipsadidae and Pseudoxenodontidae, whereas the concatenation tree inferred the Dipsadidae–Pseudoxenodontidae and Natricidae lineages to be sequential outgroups of the clade comprising all other colubroid lineages. For the species tree and concatenation tree, inferred evolutionary relationships also differed among *Pantherophis*–*Pituophis*, *Ptyas* and *Scolecophis*–*Tantilla* lineages (in Colubridae); among *Elapoidea*, *Hemibungarus*–*Naja*–*Ophiophagus*, *Micrurus* and *Hydrophis*–*Emydocephalus*–*Notechis*–*Pseudonaja*–*Laticauda* lineages (in Elapidae); among *Crotalus adamanteus*, *Crotalus pyrrhus*, *Crotalus tigris* and *Crotalus viridis* (in Viperidae); among *Buhoma*, Atractaspididae, Lamprophiidae, Prosymnidae, Psammophiidae, Pseudaspididae and Pseudoxyrhophiidae lineages (in Elapoidea). The optimal phylogenetic network inferred from our SNaQ analyses in ‘capushe’ was the network selected under the Djump algorithm, and did not include any reticulations (electronic supplementary material, table S5).

Gene trees were usually topologically consistent with the species tree and concatenation tree (mean QDiv = 0.82 between gene trees and the species tree; mean QDiv = 0.82 between gene trees and the concatenation tree). Low conflict among gene trees and each multi-locus tree was also reflected in gene concordance and discordance factors inferred at nodes of the species and concatenation trees, such that gCF was usually higher than either of gDF1 and gDF2. For the species tree, gCF  $>$  gDF1 and gCF  $>$  gDF2 except at five nodes: (i) MRCA of Lamprophiidae and Pseudoxyrhophiidae; (ii) MRCA of Lamprophiidae and Pseudaspididae; (iii) MRCA of *C. tigris* and *C. viridis*; (iv) MRCA of Dipsadidae and Natricidae; and (v) MRCA of Colubridae and Grayiidae. For the concatenation tree, gCF  $>$  gDF1 and gCF  $>$  gDF2 except at five nodes: (i) MRCA of *C. pyrrhus* and *C. viridis*; (ii) MRCA of *Hydrophis* and *Ophiophagus*; (iii) MRCA of *Elapoidea* and *Micrurus*; (iv) MRCA of Colubridae and Grayiidae; and (v) MRCA of *Pantherophis*, *Pituophis* and *Ptyas*. For both the species tree and concatenation tree, sDF1 and sDF2 significantly differed in 0.05% of 6400  $\chi^2$ -tests (64 nodes; 100 bootstraps) and never significantly differed at the same node in more than one bootstrap, consistent with ILS-only discordance expectations; gDF1 and gDF2 significantly differed at 48% or 37% of nodes of the species tree or concatenation tree, respectively (electronic supplementary material, figure S2).

Our Sanger phylogeny, estimated from analysis of our Sanger sequence dataset, included 448 tips (individuals) sampled from 432 species and 378 genera, and was strongly supported (UFBoot  $\geq 95$ ) at 60% of nodes ( $n = 327$ ) that were topologically unconstrained during phylogenetic analysis.

### 3.3. Divergence times

For lineages sampled in both our inferred species tree and Sanger tree, estimates of divergence times (means and limits of CIs) were generally older in the species tree than in the Sanger tree, especially at deeper nodes, even though node-calibrations were identical and tree topologies were consistent. Age estimates were similar between these trees at crown nodes of Colubroidea (species tree CI: 36.39–48.81 Ma; Sanger tree CI: 31.13–44.33 Ma), Elapoidea (species tree CI: 35.63–45.92 Ma; Sanger tree CI: 28.94–41.24 Ma) and for colubroid and elapoid sublineages (figures 3 and 4). The greater number of lineages sampled in the Sanger tree compared with the species tree, fewer loci sampled and inclusion of mitochondrial loci in the Sanger dataset (versus thousands of loci, all from the nuclear genome, sampled in the sequence capture dataset used to estimate divergence times for the species

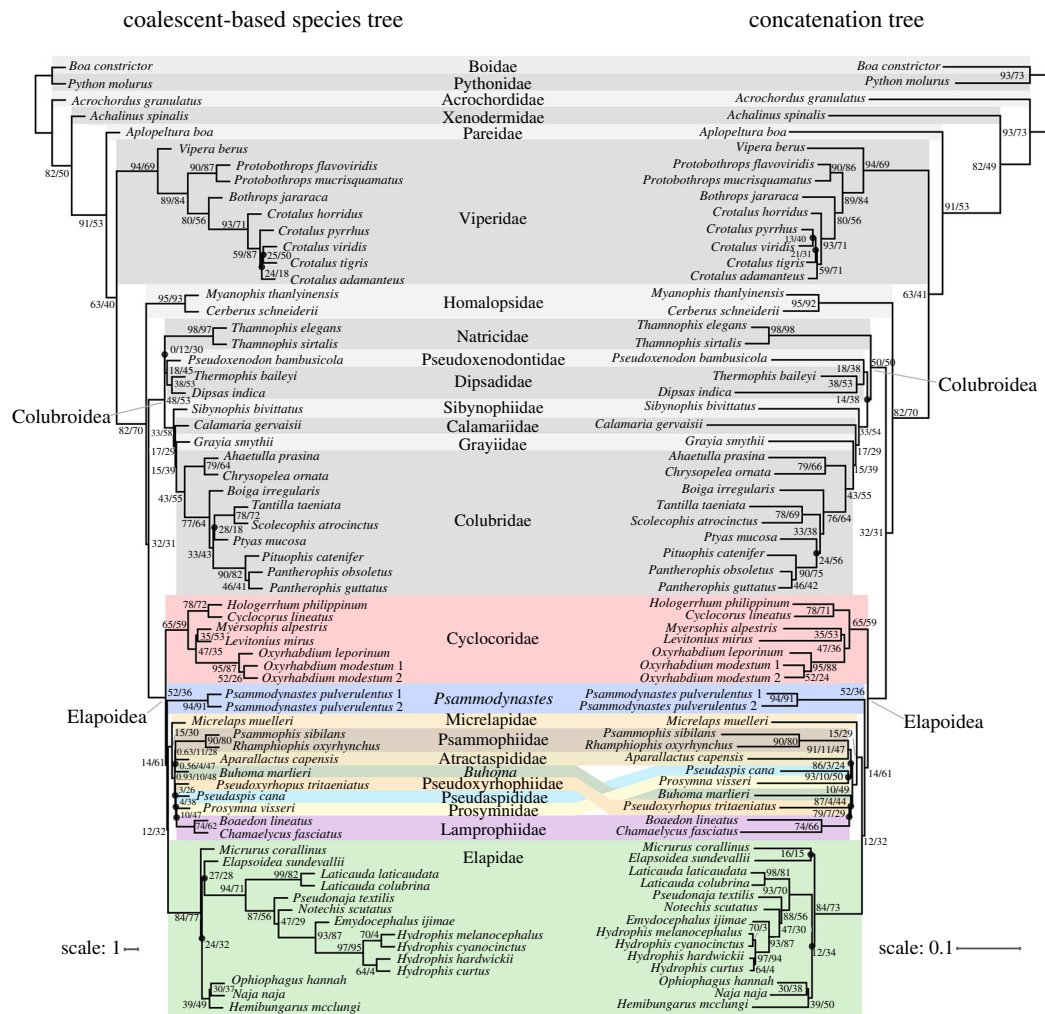


**Figure 2.** Coalescent-based species tree (left) and maximum-likelihood concatenation tree (right). Black circles indicate groups unique to either the species tree or concatenation tree. Two node values indicate gCFs/sCFs, and strong support for group monophyly ( $LPP \geq 0.95$  for species tree;  $UFBoot \geq 95$  for concatenation tree); three node values indicate ' $LPP/gCF/sCF$ ' (species tree) or ' $UFBoot/gCF/sCF$ ' (concatenation tree). Branch lengths are in coalescent units (species tree) or substitutions per site (concatenation tree).

tree) probably explain the differences in divergence times estimated for the species tree and Sanger tree. After pruning our time-calibrated Sanger phylogeny to include one tip per genus of superfamilies Colubroidea and Elapoidea, the chronogram used for biogeographic inference contained 311 tips.

### 3.4. Biogeography

Results of biogeographic analyses supported an Asian origin for both Colubroidea and Elapoidea under all biogeographic models (figure 4; electronic supplementary material, materials S3–S8). Statistical comparison of results supported the BAYAREALIKE+J as the optimal biogeographic model ( $AIC = 551$ ). Under this model (figure 4; electronic supplementary material, figure S3), our results supported multiple successful colonizations by ancestral colubroid or elapoid lineages from Asia into Africa ( $n = 15$ ), the Americas ( $n = 6$ ), Australasia ( $n = 4$ ) or Europe ( $n = 5$ ); from Africa into Asia ( $n = 7$ ), Europe ( $n = 6$ ), Australasia ( $n = 1$ ); from Europe into Asia ( $n = 1$ ); from land habitats in Australasia to marine habitats ( $n = 2$ ); and into Europe by ancestral colubroid lineages that were inferred as being widely distributed across Africa and Asia ( $n = 2$ ). Possibly, the result of our lower sampling of Old World versus New World ratsnakes (Coronellini), all models supported a single colonization event from the Americas into Europe and Africa by an ancestor of *Coronella* (Colubridae), which we consider unlikely compared with an alternative scenario involving colonization by ancestral *Coronella* from Asia

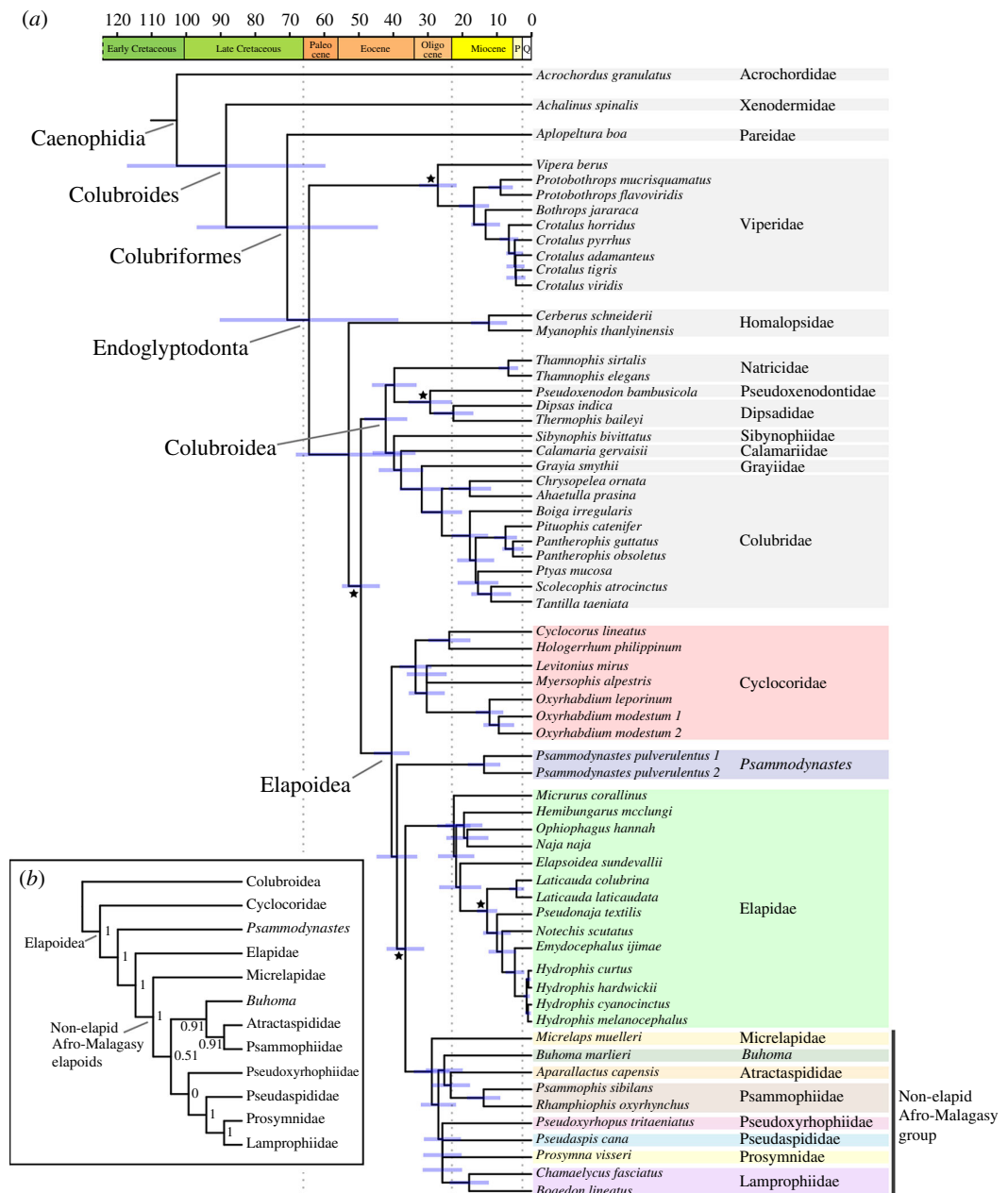


**Figure 3.** Coalescent-based species tree (a) with divergence times estimated from maximum-likelihood node dating and time scale in millions of years, and cladogram (b) detailing topology of the species tree (a) for lineages of Elapoidea. Black stars indicate fossil calibrated nodes; blue bars indicate divergence time confidence intervals; P = Pliocene epoch; Q = Quaternary period; numbers at internal nodes of (b) indicate local PP support for monophyly and PP  $\geq 0.95$  was considered strong support. This figure was illustrated using R packages 'ggtree' 3.0.4 and 'deetree' 0.2.2 [88,89].

into Europe and Africa. This latter scenario is consistent with biogeographic results of an earlier study [92] that included species-level phylogenomic sampling for ratsnakes.

Within Elapoidea, our results supported four ‘Out of Asia’ colonization events into Africa, including: (i) by an ancestor of the Afro-Malagasy group approximately 24.4–37.5 Ma (95% CI), which spans the latest Eocene and most of the Oligocene; (ii) by an ancestor of the lineage containing African cobras (genera *Aspidelaps*, *Hemachatus*, *Naja*, *Pseudohaje* and *Walterinnesia*) approximately 12.5–23.9 Ma (early and middle Miocene); (iii) by an ancestor of African garter snakes (genus *Elapsoidea*) as early as 25.6 Ma; and (iv) by an ancestor of Mambas (genus *Dendroaspis*) as early as 18.9 Ma. After these lineages colonized and diversified within Africa, our results supported successful ‘Out of Africa’ colonization of Europe by at least one sublineage in genus *Malpolon*, as early as 17.1 Ma, and separate recolonizations of Asia by *Psammophis* (less than 17.9 Ma) and *Naja* (less than 15.1 Ma).

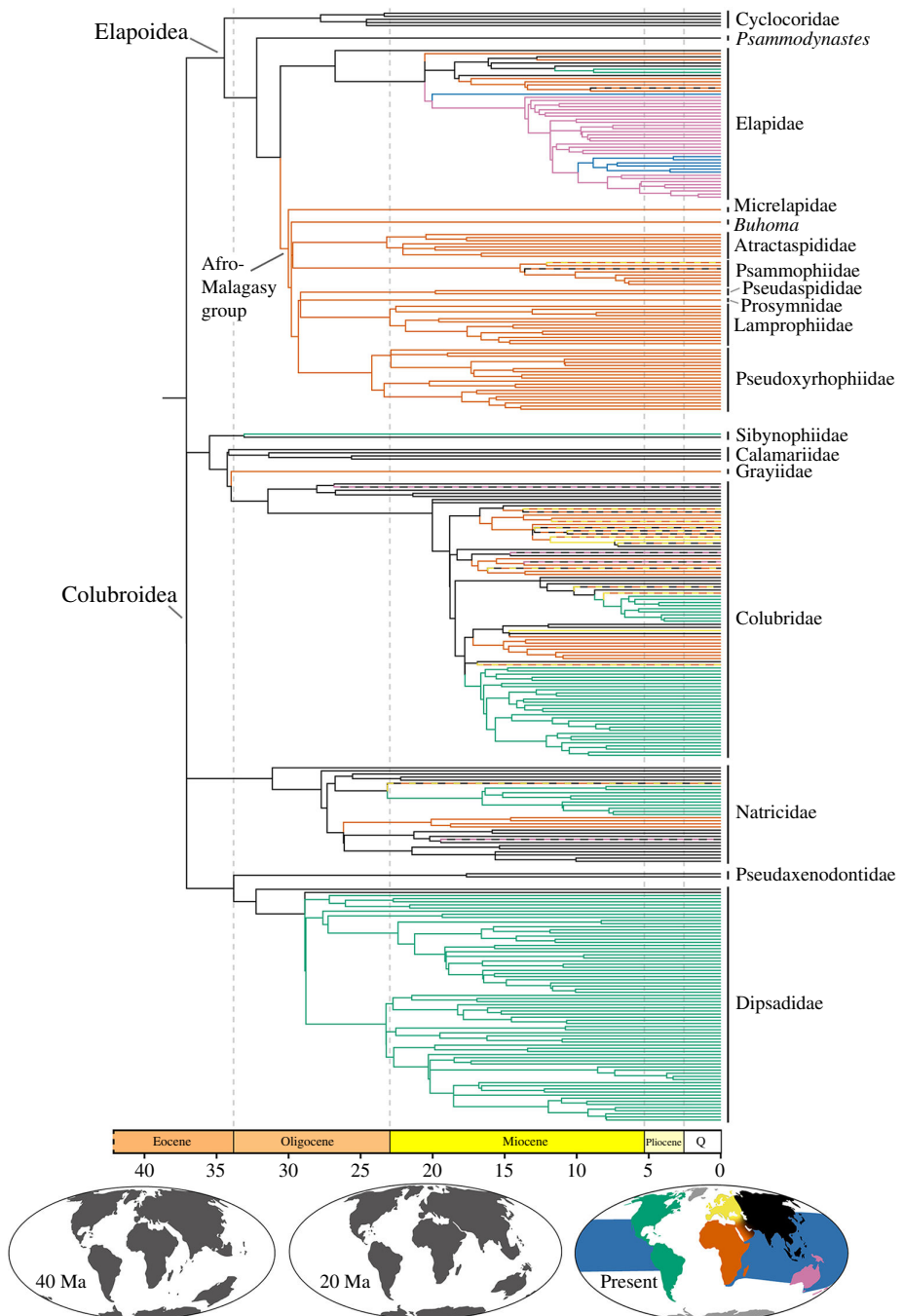


**Figure 4.** Phylogeny of Elapoidea and Colubroidea with genus-level sampling and estimates of historical geographic ranges. Branch colours correspond to colours in map and indicate maximum PP estimate of geographic range of descendant node. Time scale is in millions of years. Palaeomaps in this figure were illustrated using R packages ‘rgplates’ 0.2.0 and ‘chronosphere’ 0.4.1 [90,91].

Maximum-likelihood ancestral geographic ranges estimated with biogeographic model DIVA-LIKE+J ( $AIC = 555$ ; electronic supplementary material, figure S4) were identical to our estimates under the optimal model. Ranges estimated with model DEC+J ( $AIC = 1217$ ; electronic supplementary material, figure S5) differed from ranges estimated under the optimal model by inferring an earlier colonization of Australasia from Asia, which involved subsequent, additional colonizations from Australasia to Africa and back to Asia; and an earlier colonization of Africa, which involved an additional colonization back to Asia. Model DEC ( $AIC = 598$ ; electronic supplementary material, figure S6) supported two colonizations of Australasia by ancestral elapoids in Asia (versus one colonization under the optimal model) and two colonizations of marine environments from land habitats in Asia (versus from land habitats in Australasia under the optimal model). Furthermore, compared with our results under the optimal biogeographic model, our results under models BAYAREALIKE ( $AIC = 729$ ;

electronic supplementary material, figure S7) and DIVALIKE (AIC = 627; electronic supplementary material, figure S8) supported only one successful colonization of Africa by an elapoid: 27.9–38.6 Ma, from Asia, by an ancestor of the clade containing all elapoids except Cyclocoridae, which involved additional, subsequent colonizations of Asia from Africa.

## 4. Discussion

### 4.1. Overview

We inferred robust estimates of phylogenetic relationships and of geographic range evolution for the snake superfamily Elapoidea, a group distributed worldwide in tropical and subtropical areas that has undergone multiple rounds of rapid lineage diversification, and that includes many dangerously venomous species (e.g. cobras, coral snakes and sea snakes), as well as species that are harmless or not known to be medically significant to humans [93–95]. We generated, for the first time to date, a subgenomic (sequence capture) dataset sampling all major elapoid lineages. Our phylogenetic and divergence time estimates (figures 2 and 3) confirm early, successive divergences of the two Asia-endemic lineages, Cyclocoridae and *Psammodynastes*, within Elapoidea. Our geographic range evolution inference (figure 4) is best interpreted as supporting an Asian origin for Elapoidea, with multiple faunal exchanges between Asia and either Africa, Australasia, the Americas or Europe.

### 4.2. Biogeography

#### 4.2.1. 'Out of Africa' hypothesis is not supported for stem Elapoidea

Our phylogenetic and biogeographic results supported an Asian origin for each of superfamilies Colubroidea and Elapoidea (figure 4)—inconsistent with the 'Out of Africa' hypothesis previously suggested for Elapoidea [25] and supported in biographical literature for other vertebrate groups [30–37]. Fossil occurrences indicate an early elapoid presence in Africa: the oldest and only known Palaeogene fossils that have been interpreted as representative of Elapoidea are from southern Tanzania,  $25 \pm 0.1$  Ma, during the Late Oligocene [38,96]. As such and given the variable and conflicting phylogenetic results from earlier Sanger-based DNA sequence datasets, the Kelly *et al.* [25] 'Out of Africa' hypothesis has remained plausible. In the most recent phylogenomic studies [22,23], however, an Asian origin was supported for Elapoidea (if not discussed), given that Cyclocoridae (endemic to the Philippines) and *Psammodynastes* (endemic to eastern Asia) were recovered as the earliest branching elapoid lineages, and *Calliophis* (endemic to Asia) has been estimated often as the earliest branching lineage within Elapidae [24,26,28,97]. Our results definitively indicate an Asian origin for Elapoidea, rejecting the 'Out of Africa' hypothesis in support of the Asian origins of this group.

The absence of Palaeogene elapoid fossils outside of Africa may reflect geographic and temporal sampling gaps and uncertainty in assignment of fossils to taxonomic groups and evolutionary lineages [98]. To avoid biases associated with *a priori* misassignment of fossils to nodes or lineages during phylogenetic inference, total evidence phylogenetic dating methods for integrated analysis of molecular and morphological data have been used to jointly estimate divergence times and evolutionary relationships for extant and extinct species of other vertebrate groups [99,100], and application of these methods in future biogeographic studies of Elapoidea may provide further insight on phylogenetic relationships, divergence times and geographic range evolution in this group. Regardless, we consider our phylogenetic and biogeographic results to be strong evidence for an Asian origin for both Colubroidea and Elapoidea, a scenario that necessitates the related interpretation that numerous faunal exchanges explain the current presence of elapoid species throughout Asia, Africa, Australasia, the Americas and Europe.

#### 4.2.2. Faunal exchanges between Asia and the Americas

The modern terrestrial vertebrate fauna of the Americas includes ancient lineages that survived break-up of Laurasia or Gondwana and more recent arrivals that colonized the region by dispersal through land bridge corridors and/or over marine channels, or possibly even across open ocean [14,24,28,101–106]. Fossil evidence and molecular phylogenetic studies have supported the Bering

Land Bridge (BLB) and former North Atlantic land bridges as major dispersal corridors between Asia or Europe and the Americas, respectively [101,107–109], but whether or not these land connections were also dispersal corridors for snakes is still unclear, given that fossils of snakes are not yet known from areas coinciding with locations of former land bridges [98,110,111]. Previous phylogenetic results [101,103,112–114] and our time-calibrated phylogenomic and biogeographical range evolution results (figures 3 and 4) lend support to the interpretation of multiple colonizations from Asia, including by at least one elapoid lineage and multiple colubroid lineages. In all instances inferred here, phylogenetic relationships now firmly point to their origins in Asia, followed by separate colonizations of western North America, possibly via a BLB-facilitated overland dispersal conduit [28,112].

Land connections between western Europe and eastern North America are thought to have been submerged greater than 50 Ma [107]—prior to hypothesized colonizations by elapoid and colubroid lineages studied here (figure 3a)—whereas Beringia, during periods such as the Miocene Climatic Optimum (15–17 Ma), harboured lineages usually associated with warm climates [115–117], which may have contained habitats suitable for ectothermic vertebrates. Our phylogenetic and geographic range evolution results are consistent with historical dispersals across a Beringia land corridor, but snake fossils are not yet known from this region [98,110,111], and as such, our results cannot be interpreted as evidence against oceanic dispersal colonization [118].

#### 4.2.3. Faunal exchanges between Asia and Australasia

Hypothesized mechanisms for biotic exchange between Australasia and Asia have necessarily considered trans-oceanic dispersal, either directly or by island-hopping along intervening island chains [119,120]. Alternatively, palaeotransport, whereby lineages are thought to have rafted on drifting islands or continental fragments over geological time scales [121], may explain Asia–Australasia biotic disjunctions, as may a combination of these processes [119,122–125]. The highly dynamic, complex tectonic landscape encompassing the region between Asia and Australasia makes palaeogeographical modelling difficult [126,127], which, combined with statistical uncertainty in all estimates of lineage ages and faunal exchange times, makes it difficult to distinguish between alternative faunal exchange mechanisms between these regions. Nevertheless, our results strongly support immigration to Australasia at least once by an elapoid sublineage from Asia, and consistent with earlier studies, by multiple colubroid sublineages [36,128,129]. Our biogeographic range evolution results strongly supported successful colonization of Australasia from Asia by an ancestor of the group containing all extant Australasian elapids and sea snakes—a group classically recognized as an adaptive radiation [130,131]. Although our biogeographical range evolution results supporting two origins for extant sea snakes from ancestrally terrestrial lineages (*Hydrophiinae* and *Laticaudinae*) are consistent with the prevailing hypothesis regarding their origins, future studies should investigate whether it is appropriate to use traditional biogeographic models (e.g. DEC) for cases such as land-to-marine transitions, where colonization probably requires adaptive evolution [132–134]. Following ancestral adaptive colonizations from land to sea, both sea snake lineages further diversified in environments of the Indian and western Pacific Oceans [135,136].

#### 4.2.4. Faunal exchanges between Africa and Eurasia

Hypothesized mechanisms for Cenozoic faunal exchange between Africa and Asia or Europe have included trans-oceanic dispersal across the Tethyan Seaway, Mediterranean Sea or Indian Ocean, or dispersal across either the *Gomphotherium* land bridge resulting from Africa–Eurasia collision approximately 20 Ma [137] or an ephemeral land bridge associated with the Messinian Salinity Crisis [138–140]. Previous molecular phylogenetic studies and fossil evidence have supported a trans-Tethyan dispersal mechanism for some lizards [141], snakes [142,143], tortoises [144,145] and multiple mammal lineages [146,147]. Our biogeographic range evolution results were consistent with trans-Tethyan dispersal as the mechanism of faunal exchange only for the non-elapid Afro-Malagasy group (figure 4).

Das *et al.* [22] inferred a middle-to-late Eocene origin for the non-elapid Afro-Malagasy group, consistent with a trans-Tethys dispersal history and interpreted rapid diversification in this group as indicative of increased ecological opportunity following the Cretaceous–Palaeogene (K–Pg) mass extinction event. In contrast, our results (figures 3 and 4) and those of some earlier studies [28,148] supported more recent (late Eocene to Oligocene; 24–37 Ma) colonization and rapid diversification, and therefore, call into question previous support [22] for the K–Pg extinction-associated

ecological opportunity hypothesis. We cannot entirely reject the hypothesized association between K-Pg extinction and rapid diversification, however, and Africa is thought to have had a depauperate Palaeogene vertebrate fauna until Africa–Eurasia collision near the end of the Oligocene [137]. Additional field sampling and analyses of fossils are needed to characterize Palaeogene snake communities in Africa to better assess the long-term impacts of K-Pg extinction on species diversity, ecological opportunity and rapid diversification in lineages that subsequently colonized the continent [149,150].

Wüster *et al.* [151] inferred a mid-Eocene origin for the African cobra lineage encompassing *Aspidelaps*, *Hemachatus*, *Naja*, *Pseudohaje* and *Walterinnesia* consistent with a trans-Tethyan dispersal mechanism for their colonization, whereas our estimates support a more recent (mid-to-late Miocene; 12.5–23 Ma) arrival for cobras in Africa (figure 4), encompassing the time period when Africa and Eurasia collided and the Gomphotherium land bridge formed [152]. This land connection has been implicated as a major corridor for faunal exchange between Africa and Eurasia, which Rage and Gheerbrant [137] referred to as the Great Old World Interchange, and may have also facilitated expansions into Africa by ancestral populations of African garter snakes (*Elapoidea*) and mambas (*Dendroaspis*). After elapoid lineages successfully colonized Africa and diversified, our phylogenetic and biogeographic results (figures 3 and 4) supported multiple ‘Out of Africa’ colonizations of Asia or Europe by ancestral *Psammophis*, *Malpolon* and *Naja* sublineages.

Previous phylogenetic and phylogeographic studies have supported colonization of Asia at least twice by lineages of *Psammophis* (Psammophiidae), first by an ancestor of the clade minimally containing *P. condanarus*, *P. indochinensis*, *P. lineolatus* and *P. turpanensis*, and probably also containing *P. leithii* and *P. longifrons* [153,154]; and more recently by either an ancestor of *P. schokari* or by an ancestor of the Asian sublineage within this species [155]. Whether or not *P. leithii* and *P. longifrons* represent additional invasions of the continent must be tested with genetic data. Kurniawan *et al.* [154] hypothesized that the earlier of these *Psammophis* immigration events occurred by dispersal across the Gomphotherium land bridge, and our biogeographic and divergence time results were consistent with this hypothesis (figure 4). The importance of *Psammophis* fossils from the Late Miocene of Spain [156]—where the genus does not presently occur—in understanding when and how ancestors of extant *Psammophis* lineages arrived in Asia is not clear.

Our estimates of divergence times and biogeographic range evolution results were also consistent with colonization of Europe by an ancestor or sublineage of *Malpolon* as early as the mid-to-late Miocene (5.5–12.3 Ma). However, this early estimate is probably an artefact of our sampling only one lineage for the genus. Previous phylogeographic studies that had dense geographic genetic sampling supported multiple recent arrivals of the genus into Europe, including at least once by a sublineage of *M. monspessulanus*, probably across the Strait of Gibraltar during the Pliocene or Pleistocene [157], and separately during the Pleistocene by a sublineage of *M. insignatus* along a route east of the Mediterranean Sea [158]. Additional biotic exchanges between Africa and Eurasia have been supported for numerous vertebrate lineages during the late Miocene, and may have been facilitated by the presence of volcanic island arcs [138] and ephemeral land bridges spanning the Mediterranean during the Messinian Salinity Crisis [139,140]. The propensity of snakes for over-water dispersal, as suggested by their current presence on many oceanic islands [7,77,78,81,159–162], suggests that additional oceanic dispersal-facilitated colonizations may have occurred over deep time by lineages that have since gone extinct.

#### 4.3. Phylogenetic relationships

Our robust estimate of evolutionary relationships (figure 2) is the first to include all major lineages of Elapoidea (earlier studies did not include *Buhoma*, *Micrelaps* and *Psammodynastes* together in a phylogenomic dataset) and is congruent with phylogenetic results of several recent studies that sampled hundreds or thousands of loci [22,23,27]. Our phylogenetic results provide additional, strong statistical support for monophyly of the ‘Afro-Malagasy group’ comprising 330 species with a diversity of phenotypes and ecologies (figures 2 and 3).

On the basis of their phylogenetic results and interpretation of skeletal synapomorphies uniting *Micrelaps* and *Brachyophis* (no molecular data yet exist for the latter genus), Das *et al.* [22] proposed a new taxonomic family, Micrelapidae, within which they included *Micrelaps* and *Brachyophis*. Our phylogenetic results, which inferred *Micrelaps* as the earliest diverging lineage within the Afro-Malagasy group, were congruent with results of Das *et al.* [22], and therefore, we also recognize

*Micrelapidae* as a family-level lineage. We are preparing a manuscript to formally establish family-rank taxonomic groups for *Buhoma* and *Psammodynastes*, considering that our phylogenetic results strongly supported these taxa as lineages that are genetically distinct from each other and from other elapoid lineages.

Resolving elapoid evolutionary relationships has been notoriously difficult owing to rapid diversification in the group [22,25]—characterized in our inferred time trees by the presence of many short internal branches early in the history of the Afro-Malagasy group (figures 3 and 4). Rapid diversification is often associated with high genealogical discordance resulting from increased ILS and/or historical hybridization, prevalent in the evolutionary history of many vertebrate groups [163–171]. Results of our ILS and hybridization analyses (electronic supplementary material, figure S2 and table S5) were consistent with ILS-driven genealogical discordance and did not support historical hybridization events between major elapoid lineages. Although hybridization has been hypothesized to contribute to rapid diversification [168], our inferred lack of support for hybridization is inconsistent with this hypothesis for Elapoidea, at least for the deeper elapoid lineages sampled herein. Erosion of genomic signatures of hybridization, however, can make detection of ancient hybridization events difficult [172].

#### 4.4. Future directions

Future investigations of elapoid evolutionary relationships, divergence times and ancestral geographic ranges should use phylogenomic datasets that include more species to assess prevalence of historical hybridization, because hybridization can impact evolutionary relationships inferred using tree-based phylogenetic methods and downstream inferences from results of ancestral biogeographic reconstruction analyses. To assess whether extinct lineages (represented in the fossil record) can be included in robust phylogenetic estimates, integrative phylogenetic analysis using molecular and morphological datasets should be explored. Considering that most extinct snake species are known only from isolated vertebra, investigations should assess whether vertebral elements contain enough phylogenetic signal for robust phylogenetic inference, as previously suggested by Smith and Georgalis [98].

Our time-calibrated phylogenetic estimates and ancestral geographic range estimates will contribute to comprehensive investigations of historical environmental change. Such studies, if focused within hypothesized faunal exchange corridors, such as Beringia, would facilitate testing of ‘shared process’ hypotheses related to historical biotic exchange. Characterization of palaeoenvironments, increased sampling in future phylogenetic datasets of Elapoidea, and construction of large phenotypic and ecological datasets would enable tests of hypotheses related to drivers of lineage diversification.

### 5. Conclusions

Our phylogenetic results provided strong statistical support for relationships that historically have been difficult to resolve, while confirming relationships recovered in recent phylogenomic studies, highlighting the usefulness of generating phylogenomic datasets by targeting loci expected to contain high phylogenetic signal. Moreover, our results demonstrate the advantage of using phylogenomic datasets, compared with using datasets comprising a small number of easy-to-sequence ‘phylogenetic marker’ loci, when inferring relationships among lineages that rapidly diversified.

Biogeographic analyses using our improved phylogenetic estimate of relationships within Elapoidea unanimously supported an Asian origin for this diverse clade and strongly rejected the ‘Out of Africa’ scenario suggested in earlier phylogenetic studies of the group. This rejection of the ‘Out of Africa’ history in favour of the ‘Out of Asia’ history for ancestral Elapoidea largely reflects our improved estimate of evolutionary relationships in the group. Our novel biogeographic results highlight how prior phylogenetic assumptions can strongly impact ancestral reconstruction analyses. As large phylogenomic datasets become available for a broader diversity of biota, our ability to test major evolutionary and biogeographic hypotheses will drastically improve.

**Ethics.** Tissue samples were obtained using methods approved by the University of Kansas Institutional Animal Care and Use Committee.

**Data accessibility.** Raw sequence reads of targeted sequence capture data were accessioned in the NCBI Sequence Read Archive with BioProject PRJNA926108; sample and GenBank accession IDs associated with novel sequence

data are included in electronic supplementary material [173]. Sequence alignments, geographic data, and phylogenetic estimates are available in Open Science Framework project krhx3.

**Declaration of AI use.** We have not used AI-assisted technologies in creating this article.

**Authors' contributions.** J.L.W.: conceptualization, data curation, formal analysis, funding acquisition, investigation, methodology, resources, software, visualization, writing—original draft, writing—review and editing; F.T.B.: conceptualization, formal analysis, writing—review and editing; S.D.: conceptualization, writing—review and editing; R.M.B.: conceptualization, funding acquisition, resources, supervision, writing—review and editing.

All authors gave final approval for publication and agreed to be held accountable for the work performed therein.

**Conflict of interest declaration.** We declare we have no competing interests.

**Funding.** Financial support was provided by U.S. National Science Foundation grants (NSF-DEB 0073199, 0743491, 1418895, 0344430, 1654388, 1557053 and EF-0334952) to R.M.B. and NSF-DEB 2323125 to F.T.B., a University of Kansas Biodiversity Institute Panorama grant to J.L.W., and a KU Graduate Studies Doctoral Student Research Fund grant to J.L.W.

**Acknowledgements.** We thank the Philippine Department of Environment and Natural Resources (DENR) and the Biodiversity Management Bureau (BMB) for facilitating collecting and export permits necessary for components of the present study. For loans of genetic samples, we thank Aaron Bauer (Villanova University), Eli Greenbaum (University of Texas, El Paso) and Shai Meiri (Steinhardt Museum of Natural History, Tel Aviv University). We thank Jennifer Raff, Kirsten Jensen, and Rob Moyle for their input on an earlier version of this work.

## References

1. Lomolino MV, Riddle BR, Whittaker RJ. 2017 *Biogeography: biological diversity across space and time*, 5th edn. Sunderland, MA: Sinauer Associates, Inc.
2. Barbour T. 1912 A contribution to the zoögeography of the East Indian islands. *Mém. Mus. Comp. Zool. Harv. Coll.* **44**, 1–203.
3. Darlington Jr PJ. 1948 The geographical distribution of cold-blooded vertebrates. *Q. Rev. Biol.* **23**, 1–26. (doi:10.1086/396077)
4. Darwin C. 1839 *Journal of researches into the geology and natural history of the various countries visited by H.M.S. Beagle, under the command of Captain Fitzroy, R.N., from 1832 to 1836*. London, UK: Henry Colburn.
5. Wallace AR. 1869 *The Malay archipelago: the land of the Orang-utan, and the bird of Paradise. a narrative of travel, with studies of man and nature*. London: Macmillan and Company. (doi:10.5962/bhl.title.131886)
6. Wallace AR. 1876 *The geographical distribution of animals*. New York, NY: Harper & Brothers.
7. Leviton AE, Siler CD, Weinell JL, Brown RM. 2018 Synopsis of the snakes of the Philippines. *Proc. Calif. Acad. Sci. Ser. 4* **64**, 399–568.
8. Roll U *et al.* 2017 The global distribution of tetrapods reveals a need for targeted reptile conservation. *Nat. Ecol. Evol.* **1**, 1677–1682. (doi:10.1038/s41559-017-0332-2)
9. Álvarez-Carretero S, Tamuri AU, Battini M, Nascimento FF, Carlisle E, Asher RJ, Yang Z, Donoghue PCJ, Dos Reis M. 2022 A species-level timeline of mammal evolution integrating phylogenomic data. *Nature* **602**, 263–267. (doi:10.1038/s41586-021-04341-1)
10. Bravo GA, Schmitt CJ, Edwards SV. 2021 What have we learned from the first 500 avian genomes *Annu. Rev. Ecol. Evol. Syst.* **52**, 611–639. (doi:10.1146/annurev-ecolsys-012121-085928)
11. Dornburg A, Near TJ. 2021 The emerging phylogenetic perspective on the evolution of actinopterygian fishes. *Annu. Rev. Ecol. Evol. Syst.* **52**, 427–452. (doi:10.1146/annurev-ecolsys-122120-122554)
12. Hime PM *et al.* 2021 Phylogenomics reveals ancient gene tree discordance in the amphibian tree of life. *Syst. Biol.* **70**, 49–66. (doi:10.1093/sysbio/syaa034)
13. Simões TR, Pyron RA. 2021 The squamate tree of life. *Bull. Mus. Comp. Zool.* **163**, 47–95. (doi:10.3099/0027-4100-163.2.47)
14. Upham NS, Esselstyn JA, Jetz W. 2019 Inferring the mammal tree: species-level sets of phylogenies for questions in ecology, evolution, and conservation. *PLoS Biol.* **17**, e3000494. (doi:10.1371/journal.pbio.3000494)
15. Portik DM, Streicher JW, Wiens JJ. 2023 Frog phylogeny: a time-calibrated, species-level tree based on hundreds of loci and 5,242 species. *Mol. Phylogenet. Evol.* **188**, 107907. (doi:10.1016/j.ympev.2023.107907)
16. Brown JH, Lomolino MV. 1998 *Biogeography*, 2nd edn. Sunderland, MA: Sinauer Associates.
17. Diniz-Filho JAF, Loyola RD, Raia P, Mooers AO, Bini LM. 2013 Darwinian shortfalls in biodiversity conservation. *Trends Ecol. Evol.* **28**, 689–695. (doi:10.1016/j.tree.2013.09.003)
18. Hortal J, De Bello F, Diniz-Filho JAF, Lewinsohn TM, Lobo JM, Ladle RJ. 2015 Seven shortfalls that beset large-scale knowledge of biodiversity. *Annu. Rev. Ecol. Evol. Syst.* **46**, 523–549. (doi:10.1146/annurev-ecolsys-112414-054400)
19. Lomolino MV. 2004 Conservation biogeography. In *Frontiers of biogeography: new directions in the geography of nature* (eds MV Lomolino, LR Heaney), pp. 293–296. Sunderland, MA: Sinauer Associates.
20. Uetz P, Freed P, Aguilar R, Hošek J. 2022 The reptile database. See <http://www.reptile-database.org>.
21. Weinell JL, Brown RM. 2018 Discovery of an old, archipelago-wide, endemic radiation of Philippine snakes. *Mol. Phylogenet. Evol.* **119**, 144–150. (doi:10.1016/j.ympev.2017.11.004)
22. Das S *et al.* 2023 Ultraconserved elements-based phylogenomic systematics of the snake superfamily Elapoidea, with the description of a new Afro-Asian family. *Mol. Phylogenet. Evol.* **180**, 107700. (doi:10.1016/j.ympev.2022.107700)

23. Burbink FT *et al.* 2020 Interrogating genomic-scale data for Squamata (lizards, snakes, and amphisbaenians) shows no support for key traditional morphological relationships. *Syst. Biol.* **69**, 502–520. (doi:10.1093/sysbio/syz062)
24. Figueroa A, McKelvy AD, Grismer LL, Bell CD, Lailvaux SP. 2016 A species-level phylogeny of extant snakes with description of a new colubrid subfamily and genus. *PLoS One* **11**, e0161070. (doi:10.1371/journal.pone.0161070)
25. Kelly CMR, Barker NP, Villet MH, Broadley DG. 2009 Phylogeny, biogeography and classification of the snake superfamily Elapoidea: a rapid radiation in the late Eocene. *Cladistics* **25**, 38–63. (doi:10.1111/j.1096-0031.2008.00237.x)
26. Pyron RA, Burbink FT, Wiens JJ. 2013 A phylogeny and revised classification of Squamata, including 4161 species of lizards and snakes. *BMC Evol. Biol.* **13**, 93. (doi:10.1186/1471-2148-13-93)
27. Pyron RA, Hendry CR, Chou VM, Lemmon EM, Lemmon AR, Burbink FT. 2014 Effectiveness of phylogenomic data and coalescent species-tree methods for resolving difficult nodes in the phylogeny of advanced snakes (Serpentes: Caenophidia). *Mol. Phylogenet. Evol.* **81**, 221–231. (doi:10.1016/j.ympev.2014.08.023)
28. Zaher H *et al.* 2019 Large-scale molecular phylogeny, morphology, divergence-time estimation, and the fossil record of advanced caenophidian snakes (Squamata: Serpentes). *PLoS One* **14**, e0216148. (doi:10.1371/journal.pone.0216148)
29. Zheng Y, Wiens JJ. 2016 Combining phylogenomic and supermatrix approaches, and a time-calibrated phylogeny for squamate reptiles (lizards and snakes) based on 52 genes and 4162 species. *Mol. Phylogenet. Evol.* **94**, 537–547. (doi:10.1016/j.ympev.2015.10.009)
30. Sanders WJ. 2023 Evolution and fossil record of African Proboscidea. In *Evolution and fossil record of African Proboscidea*, 1st edn. Boca Raton, FL: CRC Press. (doi:10.1201/b20016). See <https://www.taylorfrancis.com/books/9781315118918>.
31. Pyron RA. 2014 Biogeographic analysis reveals ancient continental vicariance and recent oceanic dispersal in amphibians. *Syst. Biol.* **63**, 779–797. (doi:10.1093/sysbio/syu042)
32. Wang N, Kimball RT, Braun EL, Liang B, Zhang Z. 2017 Ancestral range reconstruction of Galliformes: the effects of topology and taxon sampling. *J. Biogeogr.* **44**, 122–135. (doi:10.1111/jbi.12782)
33. Sen S. 2013 Dispersal of African mammals in Eurasia during the Cenozoic: ways and whys. *Geo. Bios.* **46**, 159–172. (doi:10.1016/j.geobios.2012.10.012)
34. Pook CE, Joger U, Stümpel N, Wüster W. 2009 When continents collide: phylogeny, historical biogeography and systematics of the medically important viper genus *Echis* (Squamata: Viperidae). *Mol. Phylogenet. Evol.* **53**, 792–807. (doi:10.1016/j.ympev.2009.08.002)
35. Alencar LRV, Quental TB, Grazziotin FG, Alfaro ML, Martins M, Venzon M, Zaher H. 2016 Diversification in vipers: phylogenetic relationships, time of divergence and shifts in speciation rates. *Mol. Phylogenet. Evol.* **105**, 50–62. (doi:10.1016/j.ympev.2016.07.029)
36. Weinell JL, Barley AJ, Siler CD, Orlov NL, Ananjeva NB, Oaks JR, Burbink FT, Brown RM. 2021 Phylogenetic relationships and Biogeographic range evolution in cat-eyed snakes, *Boiga* (Serpentes: Colubridae). *Zool. J. Linn. Soc.* **192**, 169–184. (doi:10.1093/zoolinnean/zlaa090)
37. Weil S, Gallien L, Lavergne S, Börger L, Hassler GW, Nicolai MPJ, Allen WL. 2022 Chameleon biogeographic dispersal is associated with extreme life history strategies. *Ecography* **2022**, e06323. (doi:10.1111/ecog.06323)
38. McCartney JA, Bouchard SN, Reinhardt JA, Roberts EM, O'Connor PM, Mtelela C, Stevens NJ. 2021 The oldest Lamprophiid (Serpentes, Caenophidia) fossil from the late Oligocene Rukwa Rift Basin, Tanzania and the origins of African snake diversity. *Geo. Bios.* **66–67**, 67–75. (doi:10.1016/j.geobios.2020.07.005)
39. Bushnell B. 2014 Bbmap: a fast, accurate, splice-aware aligner. Lawrence Berkeley National Lab (LBNL). See <https://www.osti.gov/biblio/1241166>.
40. Chen S, Zhou Y, Chen Y, Gu J. 2018 Fastp: an ultra-fast all-in-one FASTQ preprocessor. *Bioinformatics* **34**, i884–i890. (doi:10.1093/bioinformatics/bty560)
41. Hutter CR, Cobb KA, Portik DM, Travers SL, Wood PL, Brown RM. 2022 Frogcap: a modular sequence capture probe-set for phylogenomics and population genetics for all frogs, assessed across multiple phylogenetic scales. *Mol. Ecol. Resour.* **22**, 1100–1119. (doi:10.1111/1755-0998.13517)
42. Laurence M, Hatzis C, Brash DE. 2014 Common contaminants in next-generation sequencing that hinder discovery of low-abundance microbes. *PLoS One* **9**, e97876. (doi:10.1371/journal.pone.0097876)
43. Bushnell B, Rood J, Singer E. 2017 Bbmerge: accurate paired shotgun read merging via overlap. *PLoS One* **12**, e0185056. (doi:10.1371/journal.pone.0185056)
44. Bankevich A *et al.* 2012 Spades: a new genome assembly algorithm and its applications to single-cell sequencing. *J. Comput. Biol.* **19**, 455–477. (doi:10.1089/cmb.2012.0021)
45. Safonova Y, Bankevich A, Pevzner PA. 2015 dipSPAdes: assembler for highly polymorphic diploid genomes. *J. Comput. Biol.* **22**, 528–545. (doi:10.1089/cmb.2014.0153)
46. Smit A, Hubley R, Green P. 2013 Repeatmasker Open-4.0. See <http://www.repeatmasker.org>.
47. Csárdi G, Nepusz T. 2006 The igraph software package for complex network research. *Inter. J.* 1–9.
48. R Core Team. 2022 *R: a language and environment for statistical computing*. Vienna, Austria: R Foundation for Statistical Computing. See <https://www.R-project.org/>.
49. Shen W, Le S, Li Y, Hu F. 2016 Seqkit: a cross-platform and ultrafast toolkit for FASTA/Q file manipulation. *PLoS One* **11**, e0163962. (doi:10.1371/journal.pone.0163962)
50. Katoh K, Standley DM. 2013 MAFFT multiple sequence alignment software version 7: improvements in performance and usability. *Mol. Biol. Evol.* **30**, 772–780. (doi:10.1093/molbev/mst010)

51. Pagès H, Aboyou P, Gentleman R, DebRoy S. 2021 Biostrings: efficient manipulation of biological strings. See <https://bioconductor.org/packages/Biostrings>.
52. Camacho C, Coulouris G, Avagyan V, Ma N, Papadopoulos J, Bealer K, Madden TL. 2009 BLAST+: architecture and applications. *BMC Bioinformatics* **10**, 421. (doi:[10.1186/1471-2105-10-421](https://doi.org/10.1186/1471-2105-10-421))
53. Weinell JL. 2022 Rees. See <https://github.com/JeffWeinell/REEs>.
54. Kearse M *et al.* 2012 Geneious basic: an integrated and extendable desktop software platform for the organization and analysis of sequence data. *Bioinformatics* **28**, 1647–1649. (doi:[10.1093/bioinformatics/bts199](https://doi.org/10.1093/bioinformatics/bts199))
55. Minh BQ, Nguyen MAT, von Haeseler A. 2013 Ultrafast approximation for phylogenetic bootstrap. *Mol. Biol. Evol.* **30**, 1188–1195. (doi:[10.1093/molbev/mst024](https://doi.org/10.1093/molbev/mst024))
56. Hoang DT, Chernomor O, von Haeseler A, Minh BQ, Vinh LS. 2018 Ufboot2: improving the ultrafast bootstrap approximation. *Mol. Biol. Evol.* **35**, 518–522. (doi:[10.1093/molbev/msx281](https://doi.org/10.1093/molbev/msx281))
57. Zhang C, Rabiee M, Sayyari E, Mirarab S. 2018 ASTRAL-III: polynomial time species tree reconstruction from partially resolved gene trees. *BMC Bioinformatics* **19**, 153. (doi:[10.1186/s12859-018-2129-y](https://doi.org/10.1186/s12859-018-2129-y))
58. Paradis E, Schliep K. 2019 Ape 5.0: an environment for modern phylogenetics and evolutionary analyses in R. *Bioinformatics* **35**, 526–528. (doi:[10.1093/bioinformatics/bty633](https://doi.org/10.1093/bioinformatics/bty633))
59. Smith MR. 2019 Quartet: comparison of phylogenetic trees using quartet and bipartition measures. *Zenodo*. <https://zenodo.org/records/2546850>
60. Guindon S, Dufayard JF, Lefort V, Anisimova M, Hordijk W, Gascuel O. 2010 New algorithms and methods to estimate maximum-likelihood phylogenies: assessing the performance of Phyml 3.0. *Syst. Biol.* **59**, 307–321. (doi:[10.1093/sysbio/syq010](https://doi.org/10.1093/sysbio/syq010))
61. Tamura K, Battistuzzi FU, Billing-Ross P, Murillo O, Filipski A, Kumar S. 2012 Estimating divergence times in large molecular phylogenies. *Proc. Natl Acad. Sci. USA* **109**, 19333–19338. (doi:[10.1073/pnas.1213199109](https://doi.org/10.1073/pnas.1213199109))
62. Tamura K, Tao Q, Kumar S. 2018 Theoretical foundation of the RelTime method for estimating divergence times from variable evolutionary rates. *Mol. Biol. Evol.* **35**, 1770–1782. (doi:[10.1093/molbev/msy044](https://doi.org/10.1093/molbev/msy044))
63. Tamura K, Stecher G, Kumar S. 2021 Mega11: molecular evolutionary genetics analysis version 11. *Mol. Biol. Evol.* **38**, 3022–3027. (doi:[10.1093/molbev/msab120](https://doi.org/10.1093/molbev/msab120))
64. Solís-Lemus C, Ané C. 2016 Inferring phylogenetic networks with maximum pseudolikelihood under incomplete lineage sorting. *PLoS Genet.* **12**, e1005896. (doi:[10.1371/journal.pgen.1005896](https://doi.org/10.1371/journal.pgen.1005896))
65. Bezanson J, Edelman A, Karpinski S, Shah VB. 2017 Julia: a fresh approach to numerical computing. *SIAM Rev.* **59**, 65–98. (doi:[10.1137/141000671](https://doi.org/10.1137/141000671))
66. Solís-Lemus C, Bastide P, Ané C. 2017 Phylonetworks: a package for phylogenetic networks. *Mol. Biol. Evol.* **34**, 3292–3298. (doi:[10.1093/molbev/msw235](https://doi.org/10.1093/molbev/msw235))
67. Burbrink FT, Gehara M. 2018 The biogeography of deep time phylogenetic reticulation. *Syst. Biol.* **67**, 743–744. (doi:[10.1093/sysbio/syy019](https://doi.org/10.1093/sysbio/syy019))
68. Arlot S, Brault V, Baudry JP, Maugis C, Michel B. 2016 Capushe: calibrating penalties using slope heuristics. See <https://CRAN.R-project.org/package=capushe>.
69. Baudry JP, Maugis C, Michel B. 2012 Slope heuristics: overview and implementation. *Stat. Comput.* **22**, 455–470. (doi:[10.1007/s11222-011-9236-1](https://doi.org/10.1007/s11222-011-9236-1))
70. Lanfear R. 2018 *Calculating and interpreting gene- and site-concordance factors in phylogenomics*. See [https://www.robertlanfear.com/blog/files/concordance\\_factors.html](https://www.robertlanfear.com/blog/files/concordance_factors.html).
71. Minh BQ, Hahn MW, Lanfear R. 2020 New methods to calculate concordance factors for phylogenomic datasets. *Mol. Biol. Evol.* **37**, 2727–2733. (doi:[10.1093/molbev/msaa106](https://doi.org/10.1093/molbev/msaa106))
72. Matzke NJ. 2013 Probabilistic historical biogeography: new models for founder-event speciation, imperfect detection, and fossils allow improved accuracy and model-testing. *Front. Biogeogr.* **5**, 242–248. (doi:[10.21425/F5FBG19694](https://doi.org/10.21425/F5FBG19694))
73. Matzke NJ. 2014 Model selection in historical biogeography reveals that founder-event speciation is a crucial process in Island clades. *Syst. Biol.* **63**, 951–970. (doi:[10.1093/sysbio/syu056](https://doi.org/10.1093/sysbio/syu056))
74. Weinell J. 2024 Genus-level geographic data for Elapoidea and Colubroidea used for biogeographic analysis in novel phylogenomic inference and “Out of Asia” biogeography of cobras, coral snakes, and their allies. (.) See <https://osf.io/5taqd/>.
75. Arakelyan MS, Danielyan FD, Corti C, Sindaco R, Leviton AE. 2011 *Herpetofauna of Armenia and Nagorno-Karabakh*. Ithaca, NY: Society for the Study of Amphibians and Reptiles (SSAR).
76. Charlton T. 2020 *A guide to snakes of Peninsular Malaysia & Singapore*. Kota Kinabalu, Borneo: Natural History Publications.
77. de Lang RD. 2011 *The snakes of the lesser Sunda Islands (Nusa Tenggara), Indonesia: a field guide to the terrestrial and semi-aquatic snakes of the lesser Sunda Islands with identification key*. Frankfurt am Main, Germany: Edition Chimaira.
78. de Lang R, Vogel G. 2005 *The snakes of Sulawesi: a field guide to the land snakes of Sulawesi with identification keys*. Frankfurt am Main, Germany: Edition Chimaira.
79. Latifi M. 1991 *The snakes of Iran*. Oxford, OH: Society for the Study of Amphibians and Reptiles (SSAR).
80. Stuebing RB, Inger RF, Lardner B, Aran K, Tan FL, Rasmussen A. 2014 *A field guide to the snakes of Borneo*, 2nd edn. Kota Kinabalu, Borneo: Natural History Publications.
81. Weinell JL, Hooper E, Leviton AE, Brown RM. 2019 Illustrated key to the snakes of the Philippines. *Proc. Calif. Acad. Sci. Ser.* **66**, 1–47.

82. Weinell JL, Paluh DJ, Siler CD, Brown RM. 2020 A new, miniaturized genus and species of snake (Cyclocoridae) from the Philippines. *Copeia* **108**, 144–150. (doi:10.1643/CH2020110)
83. Bosboom R, Mandic O, Dupont-Nivet G, Proust JN, Ormukov C, Aminov J. 2017 Late Eocene Palaeogeography of the proto-Paratethys sea in central Asia (NW China, Southern Kyrgyzstan and SW Tajikistan). *Geol. Soc. Lond. Spec. Publ.* **427**, 565–588. (doi:10.1144/SP427.11)
84. Poblete F *et al.* 2021 Towards interactive global paleogeographic maps, new reconstructions at 60, 40 and 20 Ma. *Earth Sci. Rev.* **214**, 103508. (doi:10.1016/j.earscirev.2021.103508)
85. Ree RH, Sanmartín I. 2018 Conceptual and statistical problems with the DEC+J model of founder-event speciation and its comparison with DEC via model selection. *J. Biogeogr.* **45**, 741–749. (doi:10.1111/jbi.13173)
86. Matzke NJ. 2022 Statistical comparison of DEC and DEC+J is identical to comparison of two ClaSSE submodels, and is therefore valid. *J. Biogeogr.* **49**, 1805–1824. (doi:10.1111/jbi.14346)
87. Akaike H. 1974 A new look at the statistical model identification. *IEEE Trans. Automat. Contr.* **19**, 716–723. (doi:10.1109/TAC.1974.1100705)
88. Gearty W. 2022 deeptime: plotting tools for anyone working in deep time. See <https://CRAN.R-project.org/package=deeptime>.
89. Yu G, Smith D, Zhu H, Guan Y, Lam TY. 2017 Ggtree: an R package for visualization and annotation of phylogenetic trees with their covariates and other associated data. *Methods Ecol. Evol.* **8**, 28–36. (doi:10.1111/2041-210X.12628)
90. Kocsis Á, Raja schoob N. 2020 Chronosphere: earth system history variables. In *GSA 2020 Connects Online*. (doi:10.1130/abs/2020AM-357374)
91. Kocsis ÁT, Raja NB. 2021 Rgplates: R interface for the Gplates web service and desktop application. See <https://CRAN.R-project.org/package=rgplates>.
92. Chen X, Lemmon AR, Lemmon EM, Pyron RA, Burbrink FT. 2017 Using phylogenomics to understand the link between Biogeographic origins and regional diversification in ratsnakes. *Mol. Phylogenet. Evol.* **111**, 206–218. (doi:10.1016/j.ympev.2017.03.017)
93. Casewell NR, Jackson TNW, Laustsen AH, Sunagar K. 2020 Causes and consequences of snake venom variation. *Trends Pharmacol. Sci.* **41**, 570–581. (doi:10.1016/j.tips.2020.05.006)
94. Oliveira AL, Viegas MF, da Silva SL, Soares AM, Ramos MJ, Fernandes PA. 2022 The chemistry of snake venom and its medicinal potential. *Nat. Rev. Chem.* **6**, 451–469. (doi:10.1038/s41570-022-00393-7)
95. Tasoulis T, Isbister GK. 2017 A review and database of snake venom proteomes. *Toxins (Basel)* **9**, 290. (doi:10.3390/toxins9090290)
96. McCartney JA, Stevens NJ, O'Connor PM. 2014 The earliest Colubroid-dominated snake fauna from Africa: perspectives from the Late Oligocene Nsungwe Formation of Southwestern Tanzania. *PLoS One* **9**, e90415. (doi:10.1371/journal.pone.0090415)
97. Lee MSY, Sanders KL, King B, Palci A. 2016 Diversification rates and phenotypic evolution in venomous snakes (Elapidae). *R. Soc. Open Sci.* **3**, 150277. (doi:10.1098/rsos.150277)
98. Smith KT, Georgalis GL. 2022 The diversity and distribution of Paleogene snakes: a review with comments on vertebral sufficiency. In *The origin and early evolutionary history of snakes* (eds DJ Gower, H Zaher), pp. 55–84. Cambridge, UK: Cambridge University Press. (doi:10.1017/9781108938891)
99. Ronquist F, Klopstein S, Vilhelmsen L, Schulmeister S, Murray DL, Rasnitsyn AP. 2012 A total-evidence approach to dating with fossils, applied to the early radiation of the Hymenoptera. *Syst. Biol.* **61**, 973–999. (doi:10.1093/sysbio/sys058)
100. Simões TR, Vernygora O, Caldwell MW, Pierce SE. 2020 Megaevolutionary dynamics and the timing of evolutionary innovation in reptiles. *Nat. Commun.* **11**, 3322. (doi:10.1038/s41467-020-17190-9)
101. Burbrink FT, Lawson R. 2007 How and when did Old World ratsnakes disperse into the New World. *Mol. Phylogenet. Evol.* **43**, 173–189. (doi:10.1016/j.ympev.2006.09.009)
102. Chen X, Huang S, Guo P, Colli GR, Nieto Montes de Oca A, Vitt LJ, Pyron RA, Burbrink FT. 2013 Understanding the formation of ancient intertropical disjunct distributions using Asian and Neotropical hinged-teeth snakes (*Sibynophis* and *Scaphiodontophis*: Serpentes: Colubridae). *Mol. Phylogenet. Evol.* **66**, 254–261. (doi:10.1016/j.ympev.2012.09.032)
103. Guo P, Liu Q, Xu Y, Jiang K, Hou M, Ding L, Pyron RA, Burbrink FT. 2012 Out of Asia: natricine snakes support the Cenozoic Beringian dispersal hypothesis. *Mol. Phylogenet. Evol.* **63**, 825–833. (doi:10.1016/j.ympev.2012.02.021)
104. Jetz W, Thomas GH, Joy JB, Hartmann K, Mooers AO. 2012 The global diversity of birds in space and time. *Nature New Biol.* **491**, 444–448. (doi:10.1038/nature11631)
105. Jetz W, Pyron RA. 2018 The interplay of past diversification and evolutionary isolation with present imperilment across the amphibian tree of life. *Nat. Ecol. Evol.* **2**, 850–858. (doi:10.1038/s41559-018-0515-5)
106. Nuñez LP, Gray LN, Weisrock DW, Burbrink FT. 2023 The phylogenomic and biogeographic history of the gartersnakes, watersnakes, and allies (Natricidae: Thamnophiini). *Mol. Phylogenet. Evol.* **186**, 107844. (doi:10.1016/j.ympev.2023.107844)
107. Brikiatis L. 2014 The De Geer, Thulean and Beringia routes: key concepts for understanding early Cenozoic biogeography. *J. Biogeogr.* **41**, 1036–1054. (doi:10.1111/jbi.12310)
108. Farmer JR *et al.* 2023 The Bering Strait was flooded 10,000 years before the Last Glacial Maximum. *Proc. Natl Acad. Sci. USA* **120**, e2206742119. (doi:10.1073/pnas.2206742119)
109. Raff J. 2022 *Origin: a genetic history of the Americas*, 1st edn. New York, NY: Twelve, Hachette Book Group.
110. Holman JA. 2000 *Fossil snakes of North America: origin, evolution, distribution, paleoecology*. Bloomington, IN: Indiana University Press.
111. Ivanov M. 2022 Miocene snakes of Eurasia: a review of the evolution of snake communities. In *The origin and early evolutionary history of snakes* (eds DJ Gower, H Zaher), pp. 85–110. Cambridge, UK: Cambridge University Press. (doi:10.1017/9781108938891)
112. Jiang D, Klaus S, Zhang YP, Hillis DM, Li JT. 2019 Asymmetric biotic interchange across the Bering land bridge between Eurasia and North America. *Natl. Sci. Rev.* **6**, 739–745. (doi:10.1093/nsr/nwz035)

113. Li JT, Wang JS, Nian HH, Litvinchuk SN, Wang J, Li Y, Rao DQ, Klaus S. 2015 Amphibians crossing the Bering Land Bridge: evidence from holartic treefrogs (*Hyla*, Hylidae, Anura). *Mol. Phylogenet. Evol.* **87**, 80–90. (doi:10.1016/j.ympev.2015.02.018)
114. Vila R *et al.* 2011 Phylogeny and palaeoecology of polyommatus blue butterflies show Beringia was a climate-regulated gateway to the New World. *Proc. R. Soc. B* **278**, 2737–2744. (doi:10.1098/rspb.2010.2213)
115. Reinink-Smith LM, Leopold EB. 2005 Warm climate in the late Miocene of the south coast of Alaska and the occurrence of Podocarpaceae pollen. *Palynol.* **29**, 205–262. (doi:10.1080/01916122.2005.9989607)
116. Wolfe JA. 1994 An analysis of Neogene climates in Beringia. *Palaeogeogr. Palaeoclimatol. Palaeoecol.* **108**, 207–216. (doi:10.1016/0031-0182(94)90234-8)
117. Herold N, Huber M, Müller RD. 2011 Modeling the Miocene climatic optimum. Part I: land and atmosphere. *J. Clim.* **24**, 6353–6372. (doi:10.1175/2011JCLI4035.1)
118. de Queiroz A. 2014 *The monkey's voyage: how improbable journeys shaped the history of life*. New York, NY: Basic Books.
119. Oliver PM, Brown RM, Kraus F, Rittmeyer E, Travers SL, Siler CD. 2018 Lizards of the lost arcs: mid-Cenozoic diversification, persistence and ecological marginalization in the West Pacific. *Proc. R. Soc. B* **285**, 20171760. (doi:10.1098/rspb.2017.1760)
120. Skeels A *et al.* 2023 Paleoenvironments shaped the exchange of terrestrial vertebrates across Wallace's line. *Science* **381**, 86–92. (doi:10.1126/science.adf7122)
121. Siler CD, Oaks JR, Welton LJ, Linkem CW, Swab JC, Diesmos AC, Brown RM. 2012 Did geckos ride the Palawan raft to the Philippines? *J. Biogeogr.* **39**, 1217–1234. (doi:10.1111/j.1365-2699.2011.02680.x)
122. Chan KO, Brown RM. 2017 Did true frogs "dispersify"? *Biol. Lett.* **13**, 20170299. (doi:10.1098/rsbl.2017.0299)
123. de Boer AJ, Duffels JP. 1996 Historical biogeography of the cicadas of Wallacea, New Guinea and the West Pacific: a geotectonic explanation. *Palaeogeogr. Palaeoclimatol. Palaeoecol.* **124**, 153–177. (doi:10.1016/0031-0182(96)00007-7)
124. Jönsson KA, Blom MPK, Päckert M, Ericson PGP, Irestedt M. 2018 Relicts of the lost arc: high-throughput sequencing of the *Eutrichomyias rowleyi* (Aves: Passeriformes) holotype uncovers an ancient biogeographic link between the Philippines and Fiji. *Mol. Phylogenet. Evol.* **120**, 28–32. (doi:10.1016/j.ympev.2017.11.021)
125. Oliver PM, Heiniger H, Hugall AF, Joseph L, Mitchell KJ. 2020 Oligocene divergence of frogmouth birds (Podargidae) across Wallace's line. *Biol. Lett.* **16**, 20200040. (doi:10.1098/rsbl.2020.0040)
126. Hall R. 2013 The palaeogeography of Sundaland and Wallacea since the late Jurassic. *J. Limnol.* **72**, 1–17. (doi:10.4081/jlimnol.2013.s2.e1)
127. Hall R. 2017 Southeast Asia: new views of the geology of the Malay archipelago. *Annu. Rev. Earth Planet. Sci.* **45**, 331–358. (doi:10.1146/annurev-earth-063016-020633)
128. Deepak V *et al.* 2022 Multilocus phylogeny, natural history traits and classification of natricine snakes (Serpentes: Natricinae). *Zool. J. Linn. Soc.* **195**, 279–298. (doi:10.1093/zoolinnean/zlab099)
129. Ruane S, Richards SJ, McVay JD, Tjaturadi B, Krey K, Austin CC. 2018 Cryptic and non-cryptic diversity in New Guinea ground snakes of the genus *Stegonotus* Duméril, Bibron and Duméril, 1854: a description of four new species (Squamata: Colubridae). *J. Nat. Hist.* **52**, 917–944. (doi:10.1080/00222933.2017.1391959)
130. Grundler MC, Rabosky DL. 2014 Trophic divergence despite morphological convergence in a continental radiation of snakes. *Proc. R. Soc. B* **281**, 20140413. (doi:10.1098/rspb.2014.0413)
131. Sanders KL, Lee MSY, Leys R, Foster R, Keogh JS. 2008 Molecular phylogeny and divergence dates for Australasian elapids and sea snakes (Hydrophiinae): evidence from seven genes for rapid evolutionary radiations. *J. Evol. Biol.* **21**, 682–695. (doi:10.1111/j.1420-9101.2008.01525.x)
132. Gutarra S, Rahman IA. 2022 The locomotion of extinct secondarily aquatic tetrapods. *Biol. Rev. Camb. Philos. Soc.* **97**, 67–98. (doi:10.1111/brv.12790)
133. Motani R, Vermeij GJ. 2021 Ecophysiological steps of marine adaptation in extant and extinct non-avian tetrapods. *Biol. Rev. Camb. Philos. Soc.* **96**, 1769–1798. (doi:10.1111/brv.12724)
134. Peng C *et al.* 2020 The genome of Shaw's sea snake (*Hydrophis curtus*) reveals secondary adaptation to its marine environment. *Mol. Biol. Evol.* **37**, 1744–1760. (doi:10.1093/molbev/msaa043)
135. Jackson TNW *et al.* 2016 Rapid radiations and the race to redundancy: an investigation of the evolution of Australian elapid snake venoms. *Toxins (Basel)* **8**, 309. (doi:10.3390/toxins8110309)
136. Sanders KL, Lee MSY, Bertozzi T, Rasmussen AR. 2013 Multilocus phylogeny and recent rapid radiation of the viviparous sea snakes (Elapidae: Hydrophiinae). *Mol. Phylogenet. Evol.* **66**, 575–591. (doi:10.1016/j.ympev.2012.09.021)
137. Rage JC, Gheerbrant E. 2020 Island Africa and vertebrate evolution: a review of data and working hypotheses. In *Biological consequences of plate tectonics* (eds GVR Prasad, R Patnaik), pp. 251–264. Cham, Switzerland: Springer International Publishing. (doi:10.1007/978-3-030-49753-8)
138. Booth-Rea G, Ranero CR, Grevemeyer I. 2018 The Alboran volcanic-arc modulated the Messinian faunal exchange and salinity crisis. *Sci. Rep.* **8**, 13015. (doi:10.1038/s41598-018-31307-7)
139. Hewitt GM. 2011 Mediterranean peninsulas: the evolution of hotspots. In *Biodiversity hotspots: distribution and protection of conservation priority areas*, pp. 123–148. New York, NY: Springer. (doi:10.1007/978-3-642-20992-5)
140. Zhao Z, Hou ZE, Li SQ. 2022 Cenozoic tethyan changes dominated Eurasian animal evolution and diversity patterns. *Zool. Res.* **43**, 3–13. (doi:10.24272/j.issn.2095-8137.2021.322)
141. Karin BR, Metallinou M, Weinell JL, Jackman TR, Bauer AM. 2016 Resolving the higher-order phylogenetic relationships of the circumtropical *Mabuya* group (Squamata: Scincidae): an out-of-Asia diversification. *Mol. Phylogenet. Evol.* **102**, 220–232. (doi:10.1016/j.ympev.2016.05.033)

142. Zaher H, Folie A, Quadros AB, Rana RS, Kumar K, Rose KD, Fahmy M, Smith T. 2021 Additional vertebral material of *Thaumastophis* (Serpentes: Caenophidia) from the early Eocene of India provides new insights on the early diversification of colubroidean snakes. *Geo. Bios.* **66–67**, 35–43. (doi:10.1016/j.geobios.2020.06.009)
143. El-Hares MA, Zaher H, El-Mekkawy D, El-Sayed S, Seiffert ER, Sallam HM. 2021 New records of legless squamates from the lowest upper Eocene deposits of the Fayum Depression, Egypt. *J. Vertebr. Paleontol.* **41**, e1992770. (doi:10.1080/02724634.2021.1992770)
144. Kehlmaier C *et al.* 2023 Ancient DNA Elucidates the lost world of western Indian Ocean giant tortoises and reveals a new extinct species from Madagascar. *Sci. Adv.* **9**, eabq2574. (doi:10.1126/sciadv.abq2574)
145. Hofmeyr MD, Vamberger M, Branch W, Schleicher A, Daniels SR. 2017 Tortoise (Reptilia, Testudinidae) radiations in Southern Africa from the Eocene to the present. *Zool. Scr.* **46**, 389–400. (doi:10.1111/zsc.12223)
146. Beard KC. 2016 Out of Asia: anthropoid origins and the colonization of Africa. *Annu. Rev. Anthropol.* **45**, 199–213. (doi:10.1146/annurev-anthro-102215-100019)
147. Mattingly S. 2022 *New Eurasian immigrants in the Late Paleogene of Africa, and the great Old World biotic interchange: a quantitative analysis of mammalian dispersal*. Lawrence, KS: University of Kansas.
148. Klein CG, Pisani D, Field DJ, Lakin R, Wills MA, Longrich NR. 2021 Evolution and dispersal of snakes across the Cretaceous–Paleogene Mass Extinction. *Nat. Commun.* **12**, 5335. (doi:10.1038/s41467-021-25136-y)
149. Feng YJ, Blackburn DC, Liang D, Hillis DM, Wake DB, Cannatella DC, Zhang P. 2017 Phylogenomics reveals rapid, simultaneous diversification of three major clades of Gondwanan frogs at the Cretaceous–Paleogene boundary. *Proc. Natl Acad. Sci. USA* **114**, E5864–E5870. (doi:10.1073/pnas.1704632114)
150. Couvreur TLP *et al.* 2021 Tectonics, climate and the diversification of the tropical African terrestrial flora and fauna. *Biol. Rev.* **96**, 16–51. (doi:10.1111/brv.12644)
151. Wüster W, Crookes S, Ineich I, Mané Y, Pook CE, Trape JF, Broadley DG. 2007 The phylogeny of cobras inferred from mitochondrial DNA sequences: evolution of venom spitting and the phylogeography of the African spitting cobras (Serpentes: Elapidae: *Naja nigricollis* complex). *Mol. Phylogenet. Evol.* **45**, 437–453. (doi:10.1016/j.ympev.2007.07.021)
152. Darin MH, Umhoefer PJ. 2022 Diachronous initiation of Arabia–Eurasia collision from eastern Anatolia to the southeastern Zagros mountains since middle Eocene time. *Int. Geol. Rev.* **64**, 2653–2681. (doi:10.1080/00206814.2022.2048272)
153. Chen M, Liu J, Cai B, Li J, Wu N, Guo X. 2021 A new species of *Psammophis* (Serpentes: Psammophiidae) from the Turpan Basin in northwest China. *Zootaxa* **4974**. (doi:10.11646/zootaxa.4974.1.4)
154. Kurniawan N, Septiadi L, Fathoni M, Wibawa GS, Thammachoti P. 2021 Out of Indochina: confirmed specimen record and first molecular identification of *Psammophis indochinensis* Smith, 1943 (Squamata, Psammophiidae) from Bali, Indonesia. *ChkLst.* **17**, 1521–1531. (doi:10.15560/17.6.1521)
155. Gonçalves DV, Martínez-Freiría F, Crochet PA, Geniez P, Carranza S, Brito JC. 2018 The role of climatic cycles and trans-Saharan migration corridors in species diversification: biogeography of *Psammophis schokari* group in North Africa. *Mol. Phylogenet. Evol.* **118**, 64–74. (doi:10.1016/j.ympev.2017.09.009)
156. Georgalis GL, Szynalar Z. 2022 First occurrence of *Psammophis* (Serpentes) from Europe witnesses another Messinian herpetofaunal dispersal from Africa – biogeographic implications and a discussion of the vertebral morphology of psammophiid snakes. *Anat. Rec.* **305**, 3263–3282. (doi:10.1002/ar.24892)
157. Machado L, Harris DJ, Salvi D. 2021 Biogeographic and demographic history of the Mediterranean snakes *Malpolon monspessulanus* and *Hemorrhois hippocrepis* across the Strait of Gibraltar. *BMC Ecol. Evol.* **21**, 210. (doi:10.1186/s12862-021-01941-3)
158. Carranza S, Arnold EN, Pleguezuelos JM. 2006 Phylogeny, biogeography, and evolution of two mediterranean snakes, *Malpolon monspessulanus* and *Hemorrhois hippocrepis* (Squamata, Colubridae), using mtDNA sequences. *Mol. Phylogenet. Evol.* **40**, 532–546. (doi:10.1016/j.ympev.2006.03.028)
159. Ali JR, Hedges SB. 2021 Colonizing the Caribbean: new geological data and an updated land-vertebrate colonization record challenge the GAARlandia land-bridge hypothesis. *J. Biogeogr.* **48**, 2699–2707. (doi:10.1111/jbi.14234)
160. de Lang R. 2013 *The snakes of the Moluccas (Maluku), Indonesia: a field guide to the land and non-marine aquatic snakes of the Moluccas with identification key*. Frankfurt am Main, Germany: Edition Chimaira.
161. McCoy M. 2006 *Reptiles of the Solomon Islands*. Sofia, Bulgaria: Pensoft.
162. Zug GR. 2013 *Reptiles and amphibians of the Pacific Islands: a comprehensive guide*. Berkeley, CA: University of California Press.
163. Alda F, Tagliacollo VA, Bernt MJ, Waltz BT, Ladt WB, Faircloth BC, Alfaro ME, Albert JS, Chakrabarty P. 2019 Resolving deep nodes in an ancient radiation of neotropical fishes in the presence of conflicting signals from incomplete lineage sorting. *Syst. Biol.* **68**, 573–593. (doi:10.1093/sysbio/syy085)
164. Chan KO, Hutter CR, Wood PL, Su YC, Brown RM. 2021 Gene flow increases phylogenetic structure and inflates cryptic species estimations: a case study on widespread Philippine puddle frogs (*Occidozyga laevis*). *Syst. Biol.* **71**, 40–57. (doi:10.1093/sysbio/syab034)
165. DeBaun D, Rabibisoa N, Raselimanana AP, Raxworthy CJ, Burbrink FT. 2023 Widespread reticulate evolution in an adaptive radiation. *Evolution* **77**, 931–945. (doi:10.1093/evolut/qpad011)
166. Karin BR, Gamble T, Jackman TR. 2020 Optimizing phylogenomics with rapidly evolving long exons: comparison with anchored hybrid enrichment and ultraconserved elements. *Mol. Biol. Evol.* **37**, 904–922. (doi:10.1093/molbev/msz263)
167. Liu L, Edwards SV. 2009 Phylogenetic analysis in the anomaly zone. *Syst. Biol.* **58**, 452–460. (doi:10.1093/sysbio/syp034)

168. Patton AH, Margres MJ, Epstein B, Eastman J, Harmon LJ, Storfer A. 2020 Hybridizing salamanders experience accelerated diversification. *Sci. Rep.* **10**, 6566. (doi:10.1038/s41598-020-63378-w)
169. Pyron RA, O'Connell KA, Lemmon EM, Lemmon AR, Beamer DA. 2022 Candidate-species delimitation in *Desmognathus* salamanders reveals gene flow across lineage boundaries, confounding phylogenetic estimation and clarifying hybrid zones. *Ecol. Evol.* **12**, e8574. (doi:10.1002/ece3.8574)
170. Whitfield JB, Kjer KM. 2008 Ancient rapid radiations of insects: challenges for phylogenetic analysis. *Annu. Rev. Entomol.* **53**, 449–472. (doi:10.1146/annurev.ento.53.103106.093304)
171. Whitfield JB, Lockhart PJ. 2007 Deciphering ancient rapid radiations. *Trends Ecol. Evol. (Amst.)* **22**, 258–265. (doi:10.1016/j.tree.2007.01.012)
172. Folk RA, Soltis PS, Soltis DE, Guralnick R. 2018 New prospects in the detection and comparative analysis of hybridization in the tree of life. *Am. J. Bot.* **105**, 364–375. (doi:10.1002/ajb2.1018)
173. Weinell JL, Burbrink FT, Das S, Brown R. 2024. Supplementary material from: Novel phylogenomic inference and 'Out of Asia' biogeography of cobras, coral snakes, and their allies. FigShare (doi:10.6084/m9.figshare.c.7385057)

## **Electronic Supplementary Material for “Novel phylogenomic inference and ‘Out of Asia’ biogeography of cobras, coral snakes, and their allies”**

**Tissues.** Tissues were collected by J. Alesio, K. E. Allen, V. Arias, R. M. Brown, W. and J. Bulalacao, L. Canseco, A. C. Diesmos, E. Ducasse, W. E. Duellman, J. B. Fernandez, E. B. Greenbaum, C. Hayden, J. Guayasamin, B. Gurubat, D. S. McLeod, J. Porras, S. Pouy, C. Raxworthy, R. Reyes, D. Roldán-Piña, E. L. Rico, M. B. Sanguila, C. D. Siler, J. E. Simmons, W. P. Tapondjou N., I. Tigulu, S. L. Travers, L. J. Welton, E. and Z. Wickham, and J. Zafe during field expeditions in Cameroon (2015, 2018), China (2006, 2007), El Salvador (2000), Ghana (1998), Paraguay (1996), Peru (1990), Philippines (2000, 2001, 2005, 2007, 2008, 2009, 2011, 2013, 2014, 2017), Solomon Islands (2016), and Thailand (2005), and deposited in the University of Kansas Biodiversity Institute, or as loans from tissue collections at University of Texas El Paso and Villanova University (Villanova, PA).

**Selecting loci to target for sequence capture.** Using a probe-based sequence capture approach, we targeted rapidly evolving exons (REEs), ultraconservative elements (UCEs), ddRAD-like loci (inferred *in-silico*), and protein-coding regions of previously identified major histo-compatibility (MHC), vision, and scalation-associated genes. To identify REEs, we used the R package REEs v1.9 [1] and 11 previously published squamate genome assemblies (<https://github.com/JeffWeinell/SnakeCap>). To select ddRAD-like loci, we used the REEs function "proposeLoci.ddRADlike" to locate 900–1000bp regions in the genome of *Thermophis baileyi* that begin and end with the *EcoRI* and *SbfI* restriction enzyme site recognition sequences (CCTGCAGG and GAATTC), respectively. To select vision loci, we used BLASTn from BLAST+ v2.9 [2] to search within sampled snake genomes for matches to probe sequences used by [3] for vision-associated genes in *Anolis*, *Columba*, *Gallus*, *Pelodiscus*, *Sceloporus*, or *Python*, and our probes corresponded to the genomic hit sequences of best matches. To select scalation loci, we used tBLASTn from BLAST+ to search for *Ophiophagus* and *Python*. Epidermal Differentiation Complex protein sequences previously identified by [4] in genomes of *T. sirtalis*, *P. mucrosquamatus*, and *C. horridus*. Furthermore, we included a subset of the UCEs of *Micrurus fulvius* from the study by [5], and 27 sequence regions corresponding to annotated major histocompatibility complex genes from the genome of *Thamnophis sirtalis*. Arbor Sciences synthesized 120nt RNA probes for our target sequences with 2x tiling and ultrastringent filtering, as a custom MyBaits 20,000 RNA-probes kit, and conducted library preparation prior to sequencing by NovoGene on an Illumina HiSeq X sequencing (dual-index, paired-end, 150 bp inserts). The optimized probe set included 20,020 probes for 3128 loci (1,517,011 nt) selected as targets: 1652 REEs, 907 UCEs, 328 ddRAD-like, 27 MHC, 119 vision, and 95 scalation loci (Open Science Framework, project krhx3).

**Geographic transition zones.** We considered two geographic transitional zones when coding taxa as present or absent in our geographic range dataset used for biogeographic range evolution analyses. One transition zone comprises the area containing Anatolia, Armenian Highlands, and Iranian Plateau, where Africa, Asia, and Europe meet. A second transition zone comprises islands of Wallacea between Asia and Australasia (figure S1). Colubroid or elapoid genera are not endemic to either transition zone [6–11], and therefore when scoring genera as present or absent in regions, we ignored portions of their ranges intersecting transition zones. For example,

genera occurring both within the Africa-Asia-Europe transition zone and in Africa outside of the transition zone were coded in our geographic range dataset as occurring only in “Africa”.

**Table S1.** Individuals sampled using targeted sequence capture (bold font) or from previously published assembled genomes. Institution and field series abbreviations: KU = University of Kansas; Steinhardt Museum of Natural History, Tel Aviv University; MCZ = Museum of Comparative Zoology; PNM = Philippine National Museum; UTEP = University of Texas, El Paso. For sequence capture data, raw reads are available in the NCBI Sequence Read Archive with BioProject ID PRJNA926108. Sequence alignments used for phylogenetic analyses are available on Open Science Framework, project krhx3. Data ID is either the NCBI BioSample accession number (SAMN numbers), NCBI genome assembly accession number (GCA numbers), or 'snake\_7C' for the *Boa constrictor* genome assembly (GigaDB repository; project: <http://dx.doi.org/10.5524/100060>).

Species	Family	voucher ID	other sample ID	data ID
<i>Acrochordus granulatus</i>	Acrochordidae	KU 302952	CDS 681	SAMN32850298
<i>Achalinus spinalis</i>	Xenodermidae	KU 312258	MCB 516	SAMN32850299
<i>Cerberus schneiderii</i>	Homalopsidae	KU 324534	CDS 5109	SAMN32850300
<i>Aplopeltura boa</i>	Pareidae	KU 315147	RMB 10058	SAMN32850301
<i>Ahaetulla prasina preocularis</i>	Colubridae	KU 323364	RMB 12330	SAMN32850302
<i>Calamaria gervaisii</i>	Calamariidae	KU 327406	ACD 1871	SAMN32850303
<i>Boiga irregularis</i>	Colubridae	KU 345021	SLT 833	SAMN32850304
<i>Scolecophis atrocinctus</i>	Colubridae	KU 289804	EBG 276	SAMN32850305
<i>Tantilla taeniata</i>	Colubridae	KU 289863	EBG 393	SAMN32850306
<i>Dipsas indica</i>	Dipsadidae	KU 214857	WED 59279	SAMN32850307
<i>Grayia smythii</i>	Grayiidae	KU 341872	RMB 19318	SAMN32850308
<i>Pseudoxenodon bambusicola</i>	Pseudoxenodontidae	KU 312221	KU-FS 734	SAMN32850309
<i>Sibynophis bivittatus</i>	Sibynophiidae	KU 309608	RMB 7779	SAMN32850310
<i>Elapoidea sundevallii</i>	Elapidae	MCZ R-190390	MCZ A-27807	SAMN32850311
<i>Micrurus corallinus</i>	Elapidae	KU 289205	JES 1814	SAMN32850312
<i>Hemibungarus mcclungi</i>	Elapidae	KU 303027	CDS 1486	SAMN32850313
<i>Buhoma marlieri</i>	incertae sedis	UTEP 22598	CFS 1528	SAMN32850314
<i>Aparallactus capensis</i>	Atractaspididae	MCZ R-193258	MCZ A-28808	SAMN32850315
<i>Cyclocorus lineatus lineatus</i>	Cyclocoridae	KU 335808	RMB 17698	SAMN32850316
<i>Oxyrhabdium leporinum</i>	Cyclocoridae	KU 346583	RMB 23647	SAMN32850318
<i>Oxyrhabdium modestum</i>	Cyclocoridae	KU 310866	CDS 3006	SAMN32850319
<i>Oxyrhabdium modestum</i>	Cyclocoridae	KU 338101	RMB 19059	SAMN32850317

<i>Levitonius mirus</i>	Cyclocoridae	PNM 9872	KU 337269	SAMN32850320
<i>Hologerrhum philippinum</i>	Cyclocoridae	KU 330752	CDS 5735	SAMN32850321
<i>Myersophis alpestris</i>	Cyclocoridae	KU 308684	ELR 1149	SAMN32850322
<i>Chamaelycus fasciatus</i>	Lamprophiidae	KU 348632	KAE 243	SAMN32850323
<i>Boaedon lineatus</i>	Lamprophiidae	no voucher	EBG 705	SAMN32850324
<i>Prosymna visseri</i>	Prosymnidae	MCZ R-190223	AMB 8075	SAMN32850325
<i>Psammophis sibilans</i>	Psammophiidae	KU 290424	RAX 2053	SAMN32850326
<i>Pseudaspis cana</i>	Pseudaspididae	no voucher	MCZ A-27068	SAMN32850327
<i>Pseudoxyrhopus tritaeniatus</i>	Pseudoxyrhophiidae	KU 340969	SML 029	SAMN32850328
<i>Rhamphiophis oxyrhynchus</i>	Rhamphiophiidae	KU 290451	RAX 2104	SAMN32850329
<i>Psammodynastes pulverulentus</i>	<i>incertae sedis</i>	KU 329686	RMB 14526	SAMN32850330
<i>Psammodynastes pulverulentus</i>	<i>incertae sedis</i>	KU 328547	DSM 1384	SAMN32850331
<i>Micrelaps muelleri</i>	Micrelapidae	SMNH TAU R-16738	TAU R-16738	SAMN32850332
<i>Boa constrictor</i>	Boidae	—	ERS218597	snake_7C
<i>Chrysopelea ornata</i>	Colubridae	—	—	GCA_018340635.1
<i>Pantherophis guttatus</i>	Colubridae	—	—	GCA_019457695.1
<i>Pantherophis obsoletus</i>	Colubridae	—	—	GCA_012654085.1
<i>Pituophis catenifer</i>	Colubridae	—	—	GCA_019677565.1
<i>Ptyas mucosa</i>	Colubridae	—	—	GCA_012654045.1
<i>Thamnophis elegans</i>	Natricidae	—	—	GCF_009769535.1
<i>Thamnophis sirtalis</i>	Natricidae	—	—	GCA_001077635.2
<i>Thermophis baileyi</i>	Natricidae	—	—	GCA_003457575.1
<i>Emydocephalus ijimae</i>	Elapidae	—	—	GCA_004319985.1
<i>Ophiophagus hannah</i>	Elapidae	—	—	GCA_000516915.1
<i>Hydrophis curtus</i>	Elapidae	—	—	GCA_019472885.1
<i>Hydrophis cyanocinctus</i>	Elapidae	—	—	GCA_019473425.1
<i>Hydrophis hardwickii</i>	Elapidae	—	—	GCA_004023765.1
<i>Hydrophis melanocephalus</i>	Elapidae	—	—	GCA_004320005.1
<i>Laticauda colubrina</i>	Elapidae	—	—	GCA_015471245.1

<i>Laticauda laticaudata</i>	Elapidae	—	—	GCA_004320025.1
<i>Naja naja</i>	Elapidae	—	—	GCA_009733165.1
<i>Notechis scutatus</i>	Elapidae	—	—	GCF_900518725.1
<i>Pseudonaja textilis</i>	Elapidae	—	—	GCF_900518735.1
<i>Myanophis thanlyinensis</i>	Homalopsidae	—	—	GCA_017656035.1
<i>Python molurus</i>	Pythonidae	—	—	GCA_000186305.2
<i>Bothrops jararaca</i>	Viperidae	—	—	GCA_018340635.1
<i>Crotalus adamanteus</i>	Viperidae	—	—	GCA_018446365.1
<i>Crotalus horridus</i>	Viperidae	—	—	GCA_001625485.1
<i>Crotalus pyrrhus</i>	Viperidae	—	—	GCA_000737285.1
<i>Crotalus tigris</i>	Viperidae	—	—	GCA_016545835.1
<i>Crotalus viridis</i>	Viperidae	—	—	GCA_003400415.2
<i>Protobothrops flavoviridis</i>	Viperidae	—	—	GCA_003402635.1
<i>Protobothrops mucrosquamatus</i>	Viperidae	—	—	GCA_001527695.3
<i>Vipera berus</i>	Viperidae	—	—	GCA_000800605.1

---

**Table S2.** Individuals with novel Sanger sequence data. Sequence alignment available on Open Science Framework, project krhx3.

taxon	voucher	field tag ID	GenBank (CYTB)	GenBank (CMOS)
<i>Acrochordus granulatus</i>	KU 302951	CDS 357	OQ290841	OQ290863
<i>Aplopeltura boa</i>	KU 319950	ACD 3924	OQ290842	OQ290864
<i>Boiga cynodon</i>	KU 344107	RMB 21632	OQ290843	OQ290865
<i>Calliophis bilineatus</i>	KU 309511	RMB 7884	OQ290844	OQ290866
<i>Cerberus schneiderii</i>	KU 302983	CDS 309	OQ290845	OQ290867
<i>Chrysopela paradisi</i>	KU 310165	RMB 8473	OQ290846	OQ290868
<i>Coelognathus erythrurus</i>	KU 303024	CDS 1126	OQ290847	OQ290869
<i>Cyclocorus nuchalis</i>	KU 334469	RMB 16039	OQ290848	OQ290870
<i>Gonyosoma oxycephalum</i>	KU 304104	RMB 5388	OQ290849	OQ290871
<i>Hemibungarus gemianulis</i>	—	CMNH H794	OQ290850	OQ290872
<i>Hologerrhum philippinum</i>	KU 328837	RMB 13628	OQ290851	OQ290873
<i>Laticauda colubrina</i>	KU 341149	SLT 197	OQ290852	—
<i>Laticauda colubrina</i>	KU 351734	NDR 145	OQ290853	OQ290874
<i>Naja samarensis</i>	KU 320521	CDS 3662	OQ290854	OQ290875
<i>Opisthotropis typica</i>	KU 327424	RMB 3111	OQ290855	OQ290876
<i>Oxyrhabdium leporinum</i>	KU 306307	CDS 1769	OQ290856	OQ290877
<i>Pseudorabdion taylori</i>	KU 327215	ACD 5357	OQ290857	OQ290878
<i>Sibynophis geminatus</i>	no voucher	ELR 198	OQ290858	OQ290879
<i>Stegonotus muelleri</i>	KU 328844	RMB 8541	OQ290859	OQ290880
<i>Trimeresurus flavomaculatus</i>	KU 310865	CDS 2895	OQ290860	OQ290881
<i>Tropidolaemus subannulatus</i>	KU 334489	RMB 16352	OQ290861	OQ290882
<i>Tropidonophis spilogaster</i>	KU 329682	RMB 14471	OQ290862	OQ290883

**Table S3.** Polymerase chain reaction and sequencing primers used in this study. Novel CYTB primers (72.15 and 987R.20) were designed using Primer3 v0.4.0 [12].

locus	primer name	sequence	direction	source
CYTB	L14910	GACCTGTGATMTGAAAACCAYCGTTGT	forward	[13]
CYTB	L14919	AACCACCGTTGTTATTCAACT	forward	[13]
CYTB	H16064	CTTGTTTACAAGAACAAATGCTTA	reverse	[13]
CYTB	H15720	TGGTGTGTTGTAATTGGTCT	reverse	[13]
CYTB	72F.18	AGCAATYCCTACTAYACAGC	forward	This study
CYTB	337F.23	TTCTGAGCAGCAACAGTAATCAC	reverse	[14]
CYTB	732R.21	YTCTGGTTAATGTGTTGKGG	forward	[14]
CYTB	987R.20	AATGGAGGTTGTTGACCAA	reverse	This study
C-MOS	S77	CATGGACTGGATCAGTTATG	forward	[15]
C-MOS	S78	CCTTGGGTGTGATTTCTCACCT	reverse	[15]

**Table S4.** Fossils used to calibrate node ages for divergence time estimation.

Fossil description	Calibrated node	Fossil age (Ma)
<i>Vipera</i> cf. <i>V. antiqua</i> Szyndlar & Böhme, 1993	stem-Viperinae	22.1
Elapidae indet. McCartney, Stevens, & O'Connor, 2014	stem-Elapidae	24.9
<i>Paleoheterodon tiheni</i> Holman, 1964	stem-Dipsadidae	12.5
Colubridae indet. Smith, 2013	stem-Colubroidea	35.2
<i>Incongruelaps iteratus</i> Scanlon, Lee, & Archer, & 2003	stem-Oxyuraninae	10

**Table S5.** Number of reticulations, complexity, and maximum pseudolikelihood of estimated phylogenetic networks; complexity (C) considered equal to number of identifiable (= number of internal branches + number of reticulations). Best model selected using slope heuristics estimated with capushe R package shown in bold, and using data-driven slope estimation (DDSE) and dimension jump (Djump) algorithms; MPL = maximum pseudolikelihood; MPL networks had at 0–4 reticulations, although maximum number of reticulations allowed was 0–9; HMAX = maximum number of reticulations allowed during network optimization; HMPL = number of reticulations in MPL tree.

HMAX	HMPL	C	MPL	Notes
0	0	9	87.172	<u>Results:</u> This was the model chosen by capushe as optimal, under the jump_model algorithm, when complexity was set to observed (rather than maximum) number of hybridizations.
1	1	10	72.340	<i>Buhoma + Elapsoidea</i> = stem <i>Psammophis + Aparallactus</i>
2	2	11	65.567	rerooting not possible
3	3	12	52.966	( <i>Elapsoidea + Aparallactus</i> = <i>Psammophis</i> ); ( <i>Boaedon</i> contribution to ancestral <i>Pseudoxyrhopus</i> ); ( <i>Psammodynastes</i> contribution to ancestral Africa-Malagasy lineage) <u>Results:</u> capushe selected this as the optimal model under both the DDSE_model and jump_model algorithms, when complexity was set to the maximum number of reticulations rather than to the observed number.
4	4	13	54.421	Re-rooting not possible on <i>Pseudoxenodon</i> , so rooted on <i>Hologerrhum</i> . <i>Hologerrhum + Elapsoidea</i> = <i>Pseudoxenodon</i> ; <i>Buhoma + Psammophis</i> = <i>Aparallactus</i> ; <i>Boaedon + Pseudaspis</i> = <i>Prosymna</i> ; <i>Boaedon + Pseudaspis + Prosymna</i> stem contributed to <i>Buhoma + Psammophis + Aparallactus</i> stem.
5	<b>3*</b>	12	52.943	Not possible to rerooot
6	<b>4*</b>	13	54.171	Not possible to rerooot; <u>Results:</u> This was the model chosen by capushe as optimal, under the DDSE_model algorithm, when complexity was set to observed (rather than maximum) number of hybridizations.
7	<b>3*</b>	12	50.547	<i>Elapsoidea + Aparallactus</i> = <i>Psammophis</i> ; <i>Prosymna + Pseudoxyrhopus</i> = <i>Boaedon</i> ; <i>Hologerrhum</i> + stem Africa-Malagasy lineage = <i>Psammodynastes</i>
8	<b>3*</b>	12	53.344	<i>Psammophis</i> + stem Africa-Malagasy lineage = <i>Elapsoidea</i> ; <i>Psammodynastes</i> contributed to <i>Hologerrhum</i> ; <i>Prosymna + Pseudoxyrhopus</i> = <i>Boaedon</i>
9	<b>3*</b>	12	50.812	<i>Hologerrhum</i> + stem-Africa Malagasy lineage = <i>Psammodynastes</i> ; <i>Prosymna + Pseudoxyrhopus</i> = <i>Boaedon</i> ; <i>Elapsoidea + Aparallactus</i> = <i>Psammophis</i> .
10	<b>3*</b>	12	50.658	identical to max H = 9 network

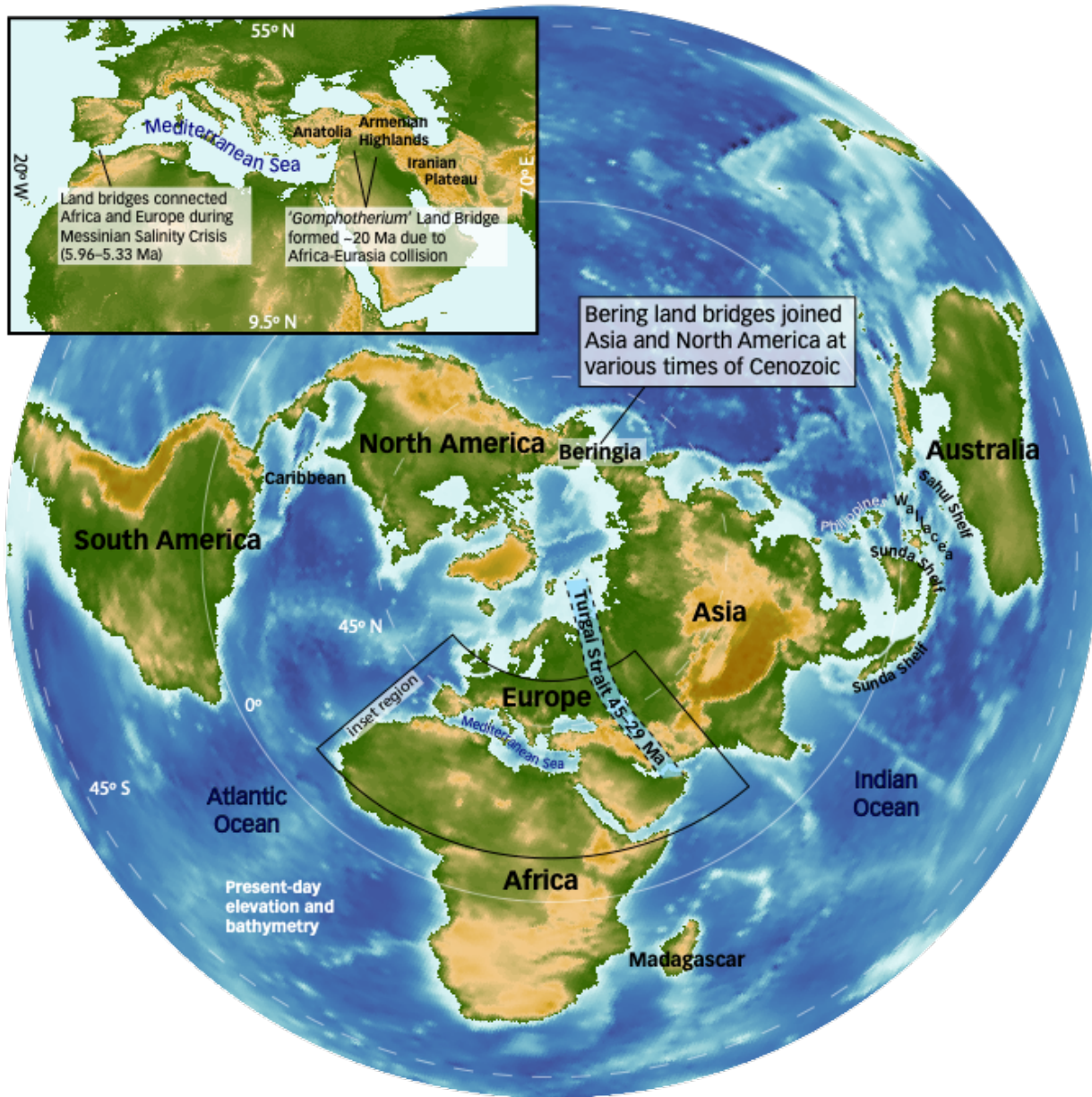


**Figure S1.** Places mentioned in this article. Colors indicate elevation above sea level (increasing from green to yellow to brown) and marine depth (blues; darker = deeper). Paleogeographical features hypothesized as facilitating or limiting historical faunal exchanges are described and indicated in the context of modern geography.

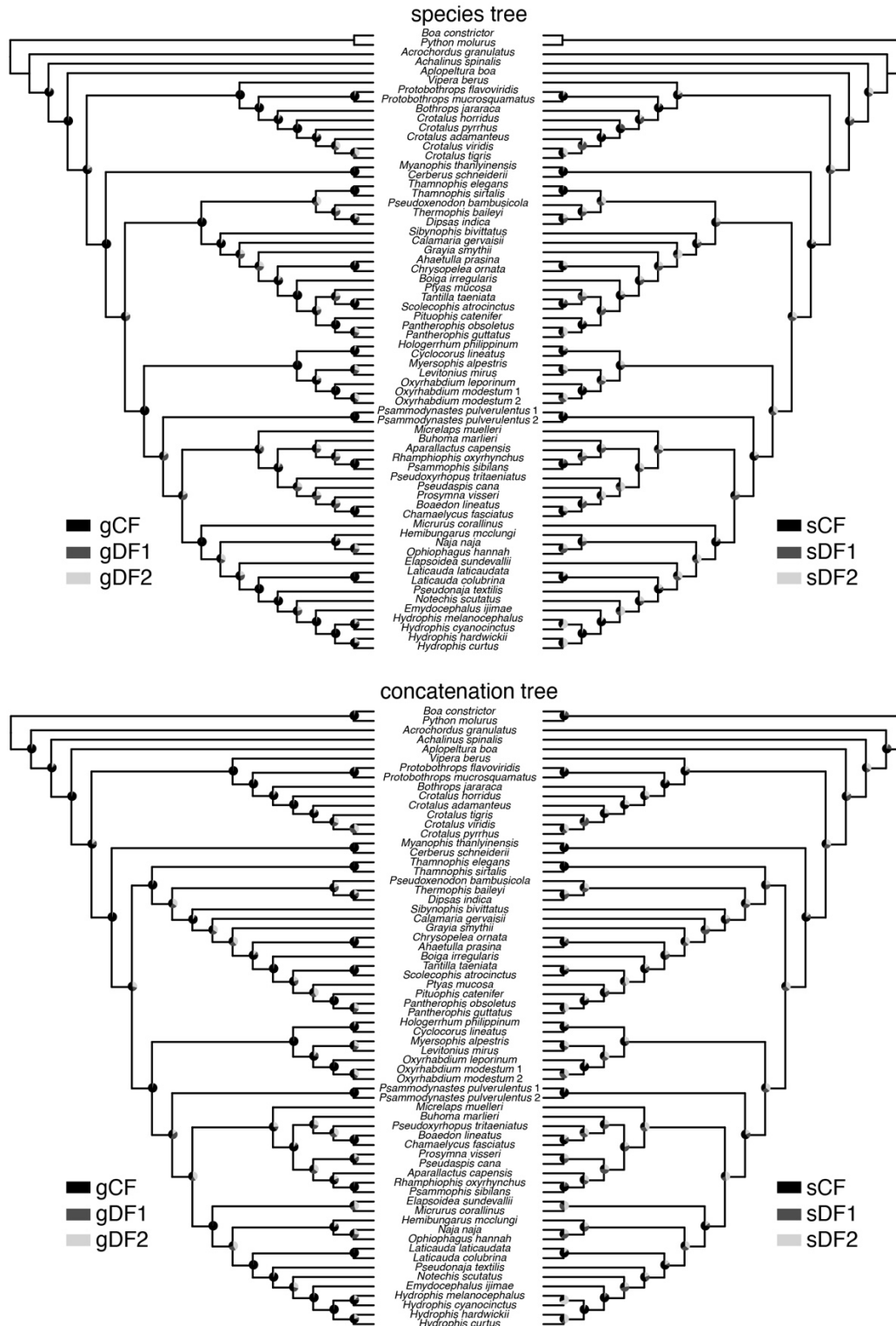


**Figure S2.** Species tree (top row) and concatenation tree (bottom row) with pie charts at nodes indicating gene (left) and site (right) concordance and discordance factors; gCF = gene concordance factor, gDF1 = gene discordance factor 1, gDF2 = gene discordance factor 2; sCF = site concordance factor, sDF1 = site discordance factor 1, sDF2 = site discordance factor 2.

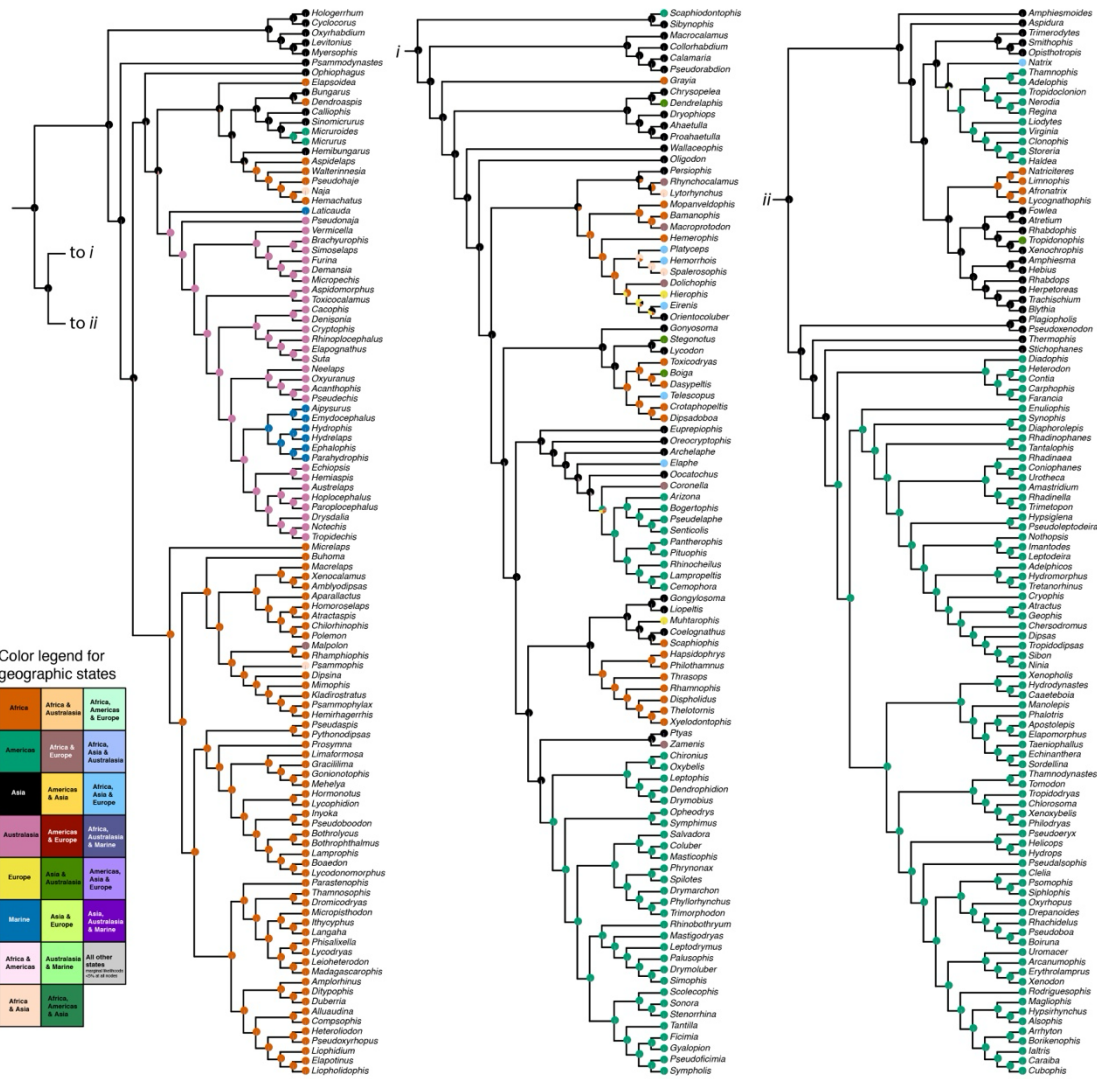


**Figure S3.** BioGeoBEARS geographic range evolution results of Elapoidea and Colubroidea under the biogeographic model “BAYAREALIKE+J”. Node pie charts depict marginal probability estimates of ancestral geographic states. Tip circles depict geographic states of extant lineages provided as input during analysis. Phylogeny used during analysis is visualized here as a cladogram.

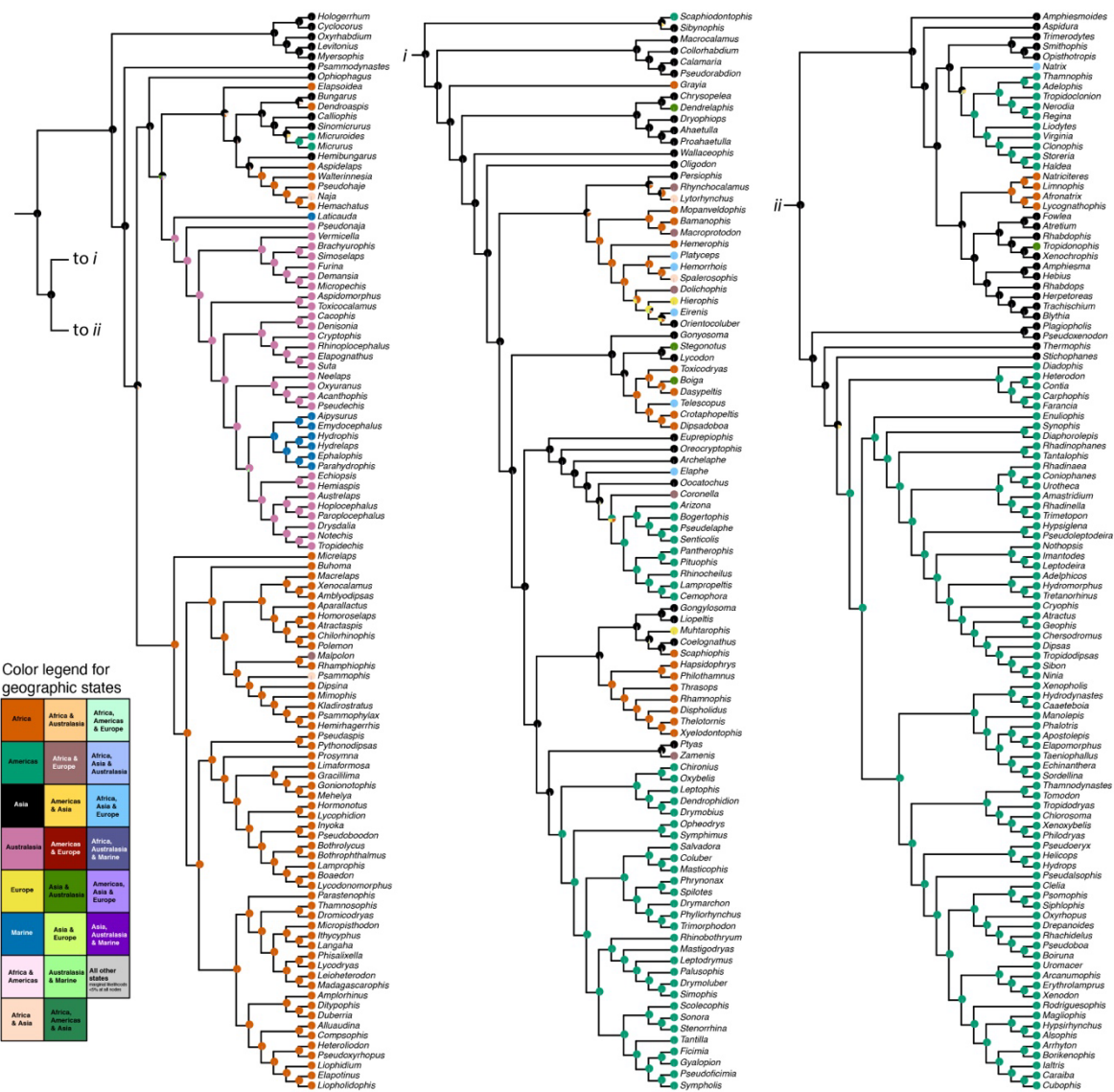


**Figure S4.** BioGeoBEARS geographic range evolution results of Elapoidea and Colubroidea under the biogeographic model “DIVALIKE+J”. Node pie charts depict marginal probability estimates of ancestral geographic states. Tip circles depict geographic states of extant lineages provided as input during analysis. Phylogeny used during analysis is visualized here as a cladogram.

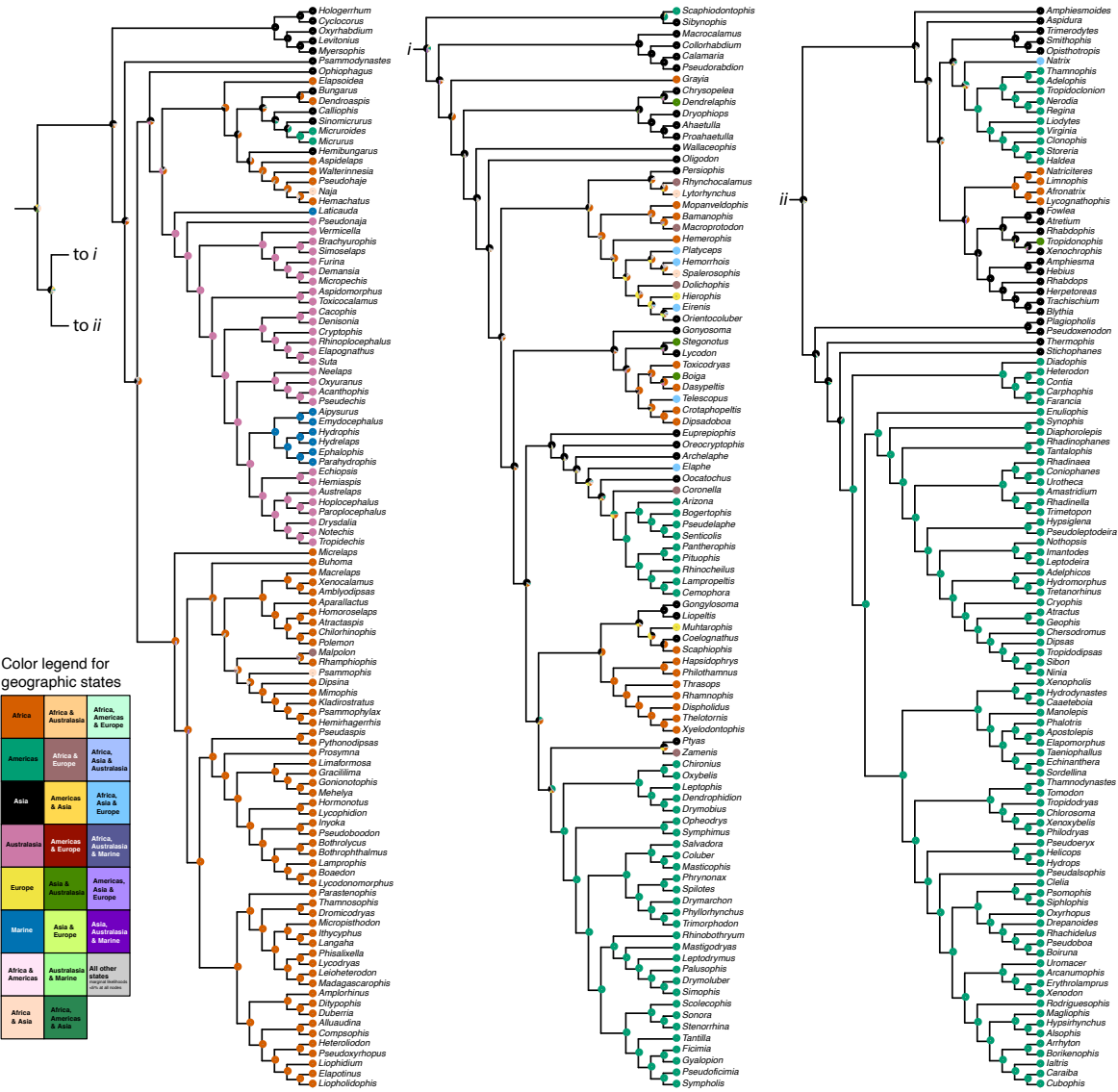


**Figure S5.** BioGeoBEARS geographic range evolution results of Elapoidea and Colubroidea under the biogeographic model “DEC+J”. Node pie charts depict marginal probability estimates of ancestral geographic states. Tip circles depict geographic states of extant lineages provided as input during analysis. Phylogeny used during analysis is visualized here as a cladogram.

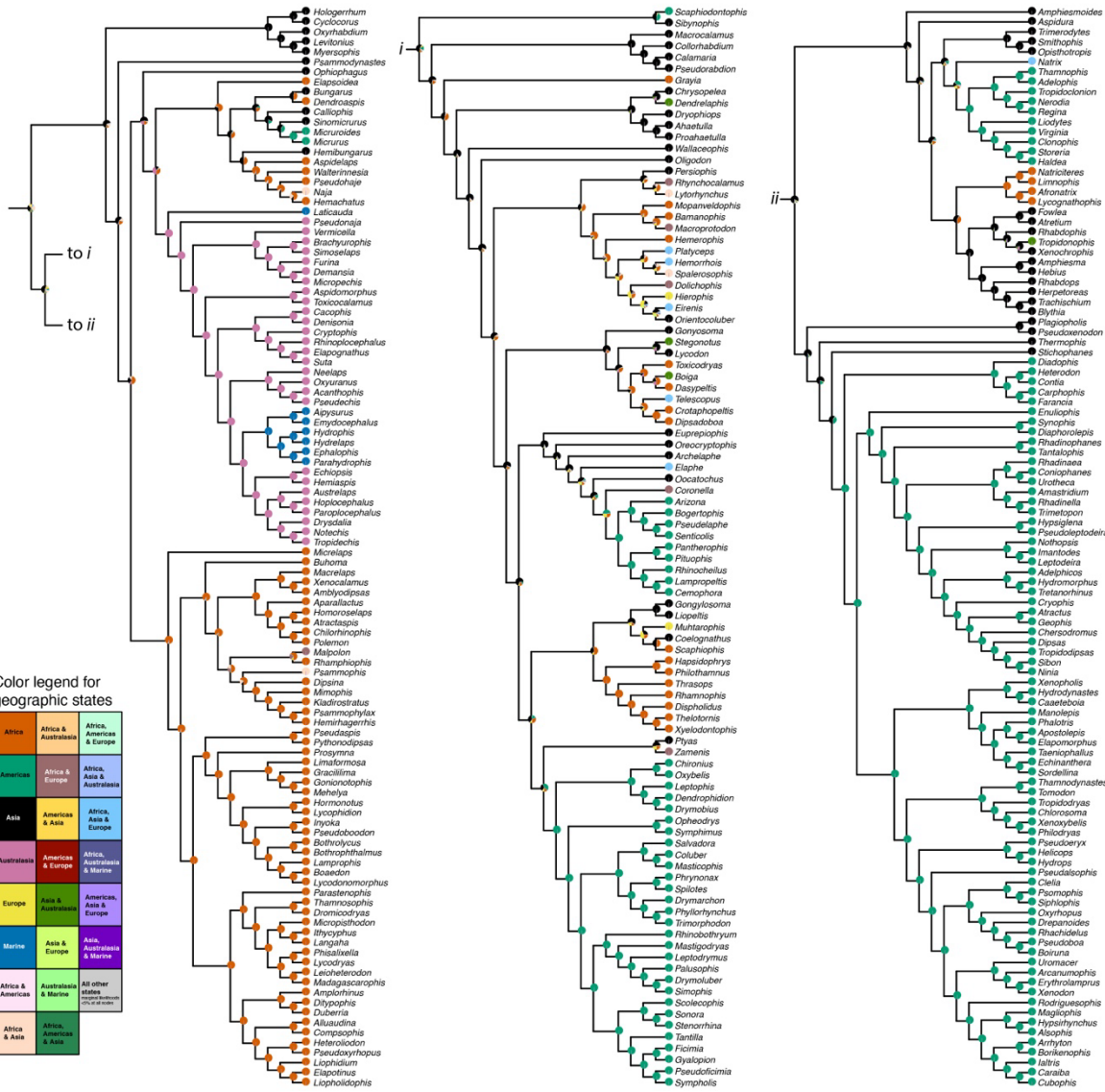


**Figure S6.** BioGeoBEARS geographic range evolution results of Elapoidea and Colubroidea under the biogeographic model “DEC”. Node pie charts depict marginal probability estimates of ancestral geographic states. Tip circles depict geographic states of extant lineages provided as input during analysis. Phylogeny used during analysis is visualized here as a cladogram.

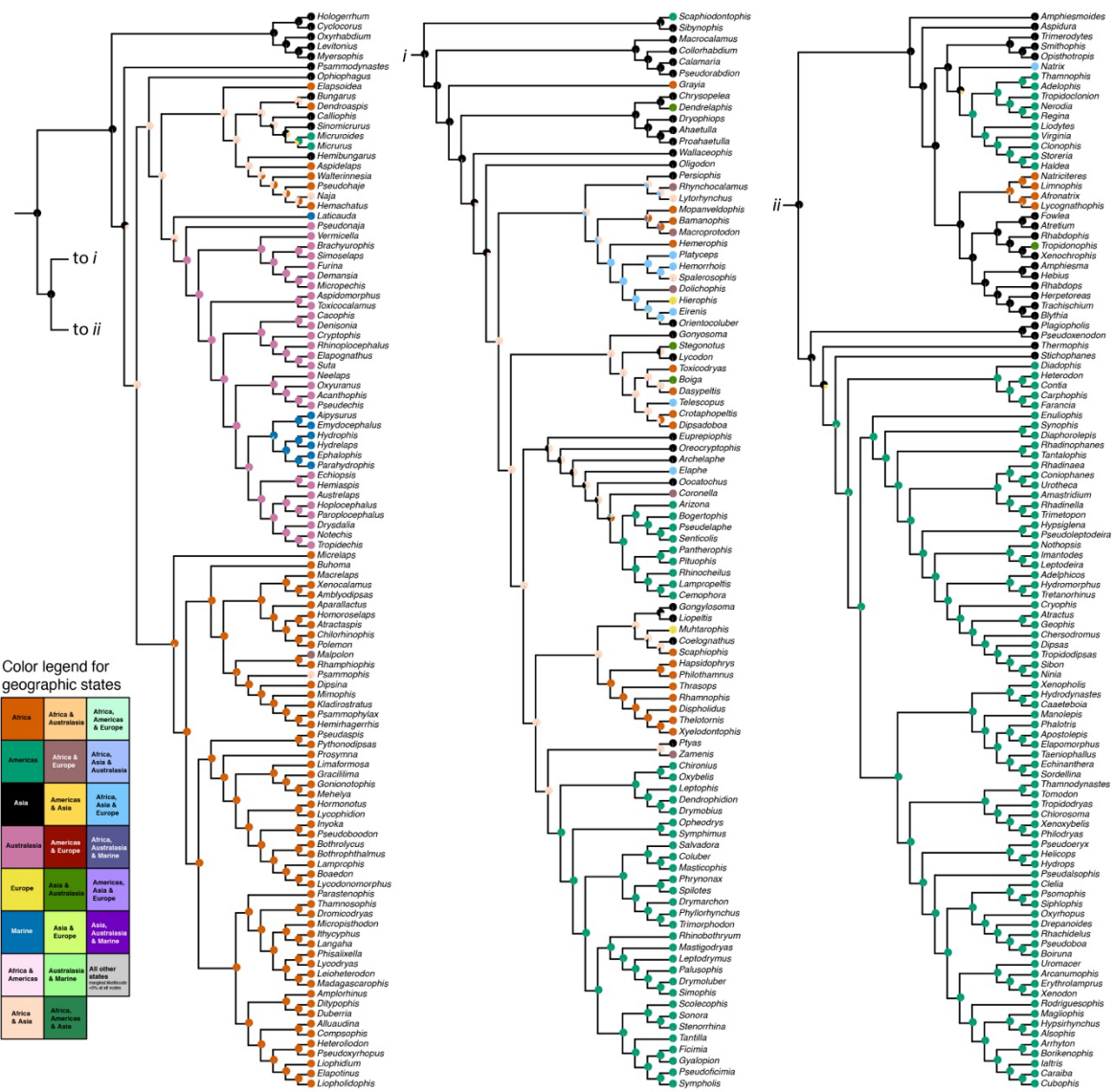


**Figure S7.** BioGeoBEARS geographic range evolution results of Elapoidea and Colubroidea under the biogeographic model “BAYAREALIKE”. Node pie charts depict marginal probability estimates of ancestral geographic states. Tip circles depict geographic states of extant lineages provided as input during analysis. Phylogeny used during analysis is visualized here as a cladogram.

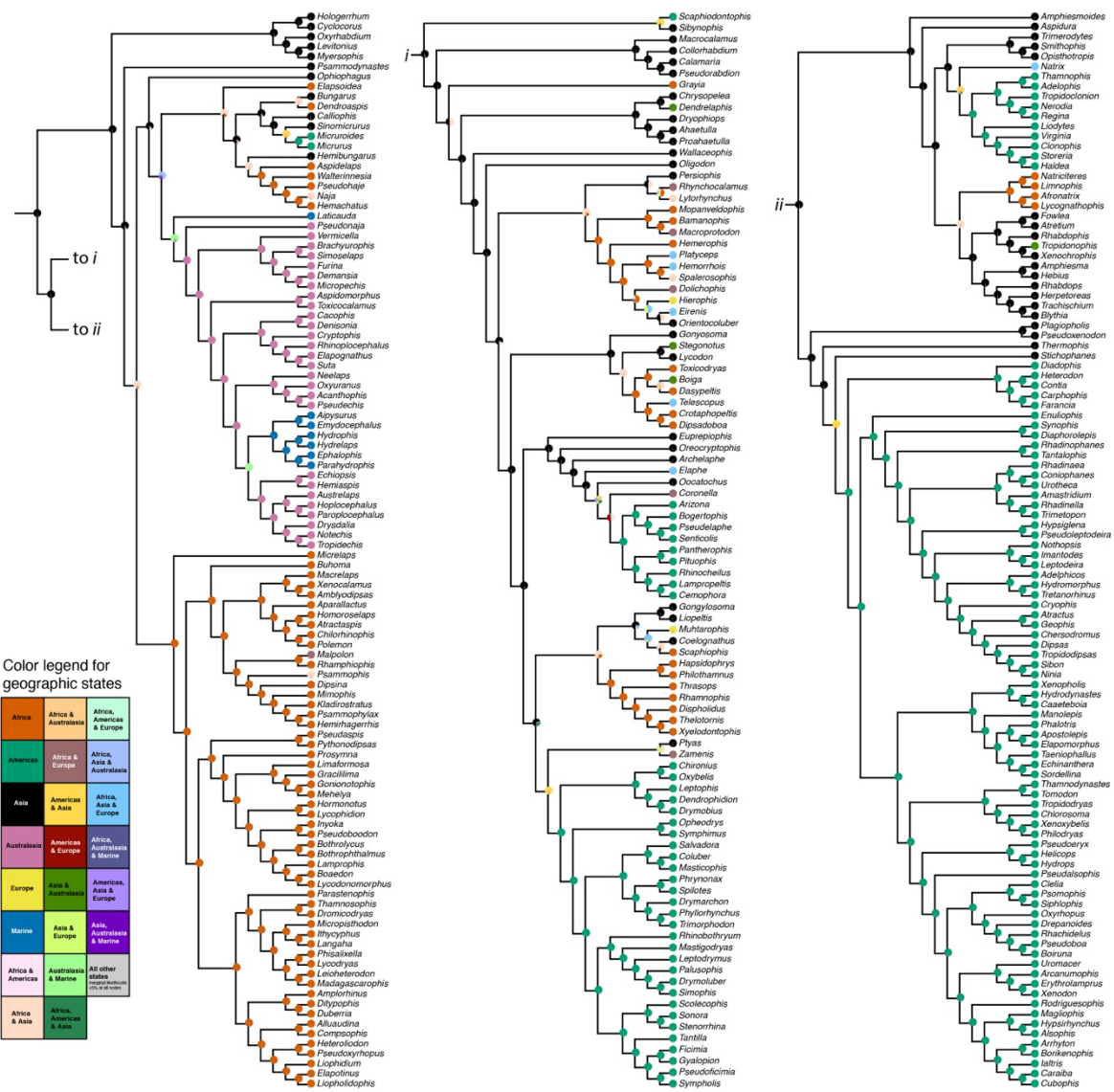


**Figure S8.** BioGeoBEARS geographic range evolution results of Elapoidea and Colubroidea under the biogeographic model “DIVALIKE”. Node pie charts depict marginal probability estimates of ancestral geographic states. Tip circles depict geographic states of extant lineages provided as input during analysis. Phylogeny used during analysis is visualized here as a cladogram.

## References

1. Weinell JL. 2022 REEs.
2. Camacho C, Coulouris G, Avagyan V, Ma N, Papadopoulos J, Bealer K, Madden TL. 2009 BLAST+: architecture and applications. *BMC Bioinformatics* **10**, 421. (doi:10.1186/1471-2105-10-421)
3. Schott RK, Panesar B, Card DC, Preston M, Castoe TA, Chang BSW. 2017 Targeted capture of complete coding regions across divergent species. *Genome Biol. Evol.* **9**, 398–414. (doi:10.1093/gbe/evx005)
4. Holthaus KB, Mlitz V, Strasser B, Tschachler E, Alibardi L, Eckhart L. 2017 Identification and comparative analysis of the epidermal differentiation complex in snakes. *Sci. Rep.* **7**, 45338. (doi:10.1038/srep45338)
5. Streicher JW, Wiens JJ. 2017 Phylogenomic analyses of more than 4000 nuclear loci resolve the origin of snakes among lizard families. *Biol. Lett.* **13**, 20170393. (doi:10.1098/rsbl.2017.0393)
6. Bar A, Haimovitch G, Meiri S. 2021 *Field guide to the amphibians and reptiles of Israel*. Frankfurt am Main: Edition Chimaira.
7. de Lang R. 2011 *The snakes of the Lesser Sunda Islands (Nusa Tenggara), Indonesia: A field guide to the terrestrial and semi-aquatic snakes of the Lesser Sunda Islands with identification key*. Frankfurt am Main: Edition Chimaira.
8. de Lang R. 2013 *The snakes of the Moluccas (Maluku), Indonesia: A field guide to the land and non-marine aquatic snakes of the Moluccas with identification key*. Frankfurt am Main: Edition Chimaira.
9. de Lang R, Vogel G. 2005 *The snakes of Sulawesi: A field guide to the land snakes of Sulawesi with identification keys*. Frankfurt am Main: Edition Chimaira.
10. Kurnaz M. 2020 Species list of amphibians and reptiles from Turkey. *J. Anim. Divers.* **2**, 10–32. (doi:10.29252/JAD.2020.2.4.2)
11. Latifi M. 1991 *The snakes of Iran*. Oxford, Ohio: Society for the Study of Amphibians and Reptiles (SSAR).
12. Untergasser A, Cutcutache I, Koressaar T, Ye J, Faircloth BC, Remm M, Rozen SG. 2012 Primer3—new capabilities and interfaces. *Nucleic Acids Res.* **40**, e115–e115. (doi:10.1093/nar/gks596)
13. Burbrink FT, Lawson R, Slowinski JB. 2000 Mitochondrial DNA phylogeography of the polytypic North American Rat Snake (*Elaphe obsoleta*): A critique of the subspecies concept. *Evolution* **54**, 2107–2118. (doi:10.1554/0014-3820(2000)054[2107:MDPOTP]2.0.CO;2)

14. Weinell JL, Paluh DJ, Siler CD, Brown RM. 2020 A new, miniaturized genus and species of snake (Cyclocoridae) from the Philippines. *Copeia* **108**, 144–150.  
(doi:10.1643/CH2020110)
15. Lawson R, Slowinski JB, Crother BI, Burbrink FT. 2005 Phylogeny of the Colubroidea (Serpentes): New evidence from mitochondrial and nuclear genes. *Mol. Phylogenet. Evol.* **37**, 581–601. (doi:10.1016/j.ympev.2005.07.016)